Characterizing carbonate reservoir fracturing from borehole data – a case study of the Viséan in northern Belgium

Eva van der Voet[1,2,*], Philippe Muchez[1], Ben Laenen[2], Gert Jan Weltje[1], David Lagrou[2] and Rudy Swennen[1]

[1] KU Leuven, Department of Earth and Environmental Sciences, Geo-institute, Celestijnenlaan 200E, B-3001 Leuven-Heverlee, Belgium

[2] Vlaamse Instelling voor Technologisch Onderzoek (VITO), Boeretang 200, B-2400 Mol, Belgium

* Corresponding author. *E-mail addresses*: eva.vandervoet@kuleuven.be and eva.vandervoet@vito.be

ABSTRACT

Fractured carbonate rocks are widely used as hydrocarbon or geothermal reservoirs. To provide a better understanding of the distribution and characteristics of such fractures, a general workflow will be presented for the characterization of fracturing from borehole data, by exploration and statistical analyses of integrated datasets. In a case study of Viséan limestones in a Belgian borehole, both cores and geophysical well logs were used to investigate which factors control the characteristics of partially open veins, which contribute to permeability. Relationships between multiple variables were tested statistically. Lithology, geochemistry and geophysical well log values were taken into account, as well as quantified veins, vugs and stylolites from cores. Although natural joint frequencies appeared hard to quantify from the available data, partially open vein characteristics could be well quantified. The results show that differential compaction controlled the development of fractures. Fracturing occurred preferentially in massive reefal buildup boundstones in contrast to layered wacke- to grainstones. Layer-parallel slip along bedding surfaces could also have reduced fracture development in the latter limestones. Frequencies of cemented veins and partially open veins are positively correlated, which suggests that the partially open veins result from either re-opening by dissolution, or (re-)opening due to a later fracturation phase. In summary, this multi-source study provides a workflow for fracture characterization from boreholes, as well as insights into the factors controlling the distribution and characteristics of partially open veins, which enhance reservoir permeability.

Keywords: borehole cores, geophysical well logs, veins, principal component analysis, fractured reservoir, differential compaction

1 INTRODUCTION

Naturally fractured carbonate rocks are often targeted as potential reservoirs for hydrocarbons or geothermal water. In the context of the global energy transition, the interest in deep geothermal energy systems is rapidly increasing. An appropriate geothermal reservoir that meets the demand is dependent on many different factors. One important factor relates to the permeability, which on itself is dependent on multiple properties. Rock fracturing is of major importance for permeability, especially in carbonate reservoirs with low primary matrix porosity and permeability (Warren & Root, 1963; Nelson, 1985). In order to reduce the risks for developing new geothermal systems in such tight reservoirs, understanding fracture characteristics and underlying processes is needed.

From a reservoir perspective, the most interesting parameter to be determined would be the distribution and connectivity of joints (non-cemented extension fractures), since these have a large effect on permeability (Warren & Root, 1963; National Research Council, 1996). Unfortunately, natural joints cannot be quantified from core material directly, since it is impossible to define the cause of a discontinuity between two core samples. Such discontinuities could also reflect drilling induced fractures (Pendexter & Rohn, 1954; Li & Schmitt, 1998) or relate to the coring process or previous research or transport activities. Some veins (cemented fractures) are partially open and could thus also contribute to permeability. These are quantifiable from cores and are the main focus of interest in this study.

In this study, the Viséan (Lower Carboniferous) limestones of the Heibaart DZH1 borehole in northern Belgium were used as a case study. This well was drilled in the Campine-Brabant Basin, a Variscan foreland basin in northern Belgium and the southern Netherlands. In the context of a geothermal project, reservoir characteristics of the carbonates are re-evaluated. The Heibaart DZH1 borehole was chosen as a case study because of the large amount of available core material, the variety of well described lithologies, the known existence of open karstic features, and the availability of multiple geophysical well logs.

To study the factors controlling the development and preservation of these partially open veins, as many variables as possible were taken into account. Four different datasets were used in the case study, regarding lithotype, geochemistry, geophysical well logs and physical features from cores. From the cores, not only partially open veins were quantified, but also features which do not directly contribute to permeability, such as cemented veins, (partially open) vugs and stylolites.

A classical approach to study fracture distributions is by ‘mechanical stratigraphy’ or ‘fracture stratigraphy’. Many studies on these topics have been carried out, based on outcrop studies (Di Naccio *et al.*, 2005; Cooke *et al.*, 2006; Jacquemyn *et al.*, 2012;

Lamarche *et al.*, 2012; Ferril *et al.*, 2017; McGinnis *et al.*, 2017; Faÿ-Gomord *et al.*, 2018) or borehole cores and geophysical well logs (Laubach *et al.*, 2009). According to Laubach *et al.* (2009), mechanical stratigraphy means the subdivision of a stratified rock sequence into mechanical units based on mechanical properties “such as tensile strength, elastic stiffness, brittleness, and fracture mechanics properties”. The authors state that fracture stratigraphy is different since it subdivides a sequence into fracture units based on “extent, intensity, or some other observed fracture attribute”. The present study deals with these fracture parameters, not with mechanical parameters.

In most of the mentioned studies, sequences were subdivided into mechanical units or fracture units based on quantified parameters such as fracture intensity/density/spacing, fracture length/height, fracture propagation or fracture orientation, often normalized for the thickness of beds or defined units. Laubach *et al.* (2009) discussed borehole studies in which fracture numbers were derived from core material or image logs. Rock property measurements of Young’s modulus and Poisson ratio were added. The present study focuses on differences and interdependencies between fracture characteristics and many different variables based on statistical analyses, instead of subdividing a single sequence into units. Furthermore, it does not only take into account the parameters that contribute directly to the permeability of a system, such as partially open veins, but also studies relationships with other features, such as veins and stylolites, which can provide information on the mechanical behavior and the diagenetic history of the rocks.

The aim of the present study is to investigate which factors control the distribution and characteristics of partially open fractures, and to which extent. This study presents a workflow for the characterization of reservoir fracturing from borehole data. Information from both core material and geophysical well logs was taken into account.

2 GEOLOGICAL SETTING

In northern Belgium, the southern part of the Netherlands and the western-most part of Germany, a vast amount of carbonates was deposited during the Lower Carboniferous, in a shallow marine basin that is mostly referred to as the Campine Basin (Ziegler, 1990; McCann, 2008) or Campine-Brabant Basin (Bless *et al.*, 1983; Muchez et al., 1987; Muchez & Viaene, 1990). In this study, we consider the Campine-Brabant Basin sensu lato (fig. 1), as a part of the Northwest European Carboniferous Basin (NWECB; Kombrink et al., 2008). The Campine-Brabant Basin is a Variscan foreland basin with a NW-SE axis which stretched from the northern flank of the London-Brabant Massif northeastward up to the (Zandvoort-)Maasbommel-Krefeld High complex in the Netherlands and Germany (Bless et al., 1983; Harings, 2014) (fig. 1). In the western part, the basin extends in the North Sea towards the United Kingdom, along the Hewett shelf and the Winterton High (Total E&P UK, 2007). In the eastern part, it extends to a small part of Germany (the Niederrheinische Bucht) and is bounded by the Midi thrust fault (Bless et al., 1983). At the southern, northeastern and possibly northern margin of the Campine-Brabant Basin, carbonate platforms were present (Kombrink et al., 2008; Geluk et al., 2007).

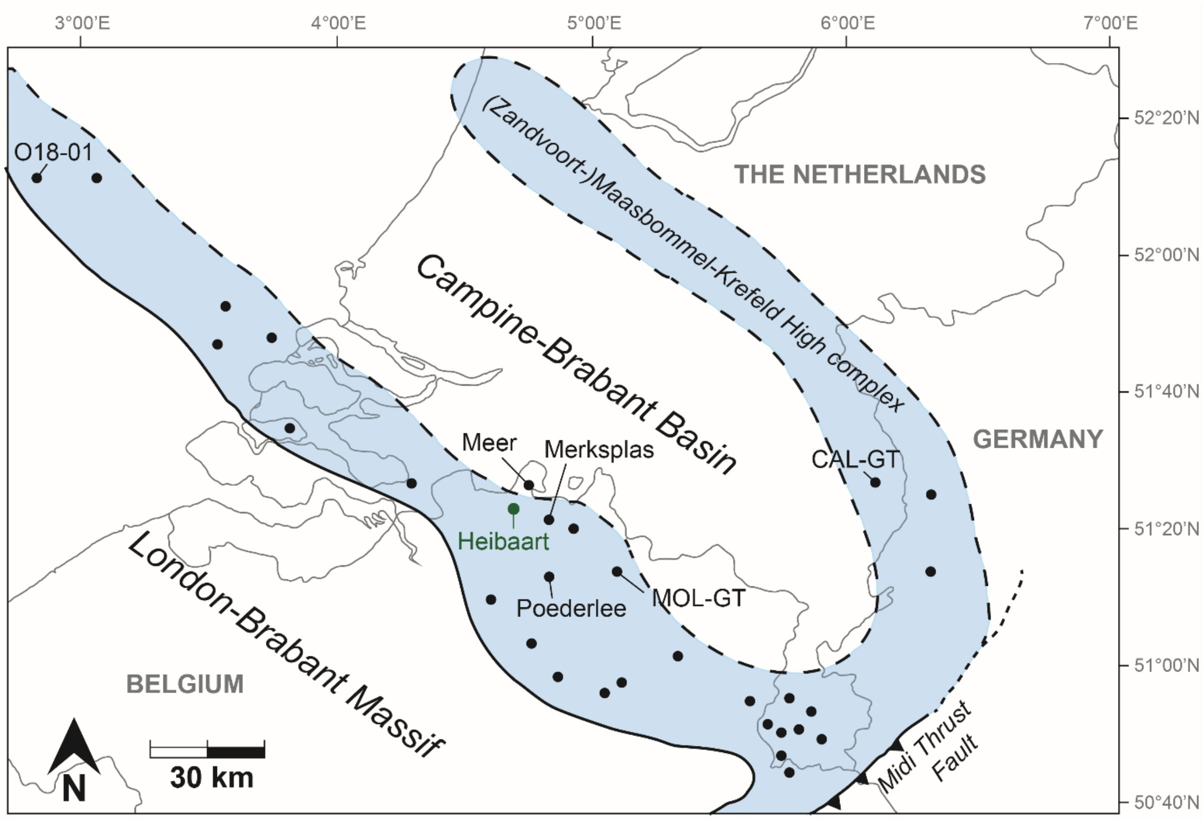

Figure 1 Map of the Campine-Brabant Basin, with well locations that transected Lower Carboniferous carbonates (black dots), the possible outlines of the carbonate ramp/shelf (dashed black line and blue fill). Modified after: Bless et al. *(1983), Muchez & Langenaeker (1993), Geluk* et al. *(2007), Kombrink* et al*. (2008), Van Hulten (2012) and Reijmer* et al. *(2017). 'Heibaart' refers to the multiple wells drilled by Distrigaz (Fluxys) at Heibaart/Loenhout, of which DZH1 is one. 'MOL-GT' and 'CAL-GT' refer to the geothermal wells drilled in Mol-Donk (Balmatt project) and Horst aan de Maas (Californië, Venlo) respectively, which are mentioned in the text.*

2.1 Structural framework

Block faulting, dominated by synsedimentary (N)NW-(S)SE trending normal faults, caused large differences in the thickness of the Viséan sequence in northern Belgium (fig. 2; Bless *et al.*, 1981; Langenaeker, 2000; Laenen et al., 2004; McCann, 2008; Bos & Laenen, 2017). This pattern was further fragmented by east-west oriented cross-faults (Langenaeker, 2000; Laenen *et al.*, 2004). Most of the faults already existed during the Carboniferous and some were reactivated during the Late Jurassic extensional Cimmerian phase, related to the opening of the Atlantic, or during the Late Cretaceous Sub-Hercynian inversion phase, related to the Alpine collision (Ziegler, 1990; Langenaeker, 2000; Laenen *et al.,* 2004). Furthermore, an east-west striking listric normal fault formed in the northern part of the Belgian Campine-Brabant Basin, approximately along the border between Belgium and the Netherlands, as a result of a N-S extensional regime during the Middle Devonian to Early Carboniferous. This north-dipping growth fault, called the Hoogstraten fault, downthrusted the Lower Carboniferous sequence (Vandenberghe, 1984; Muchez & Langenaeker, 1993; Langenaeker, 2000). The Heibaart DZH1 borehole is located on a structural high south of this Hoogstraten fault, in a fault block bounded by two NNW-SSE trending normal faults (fig. 2). This dome structure is fragmented by smaller normal faults as well.

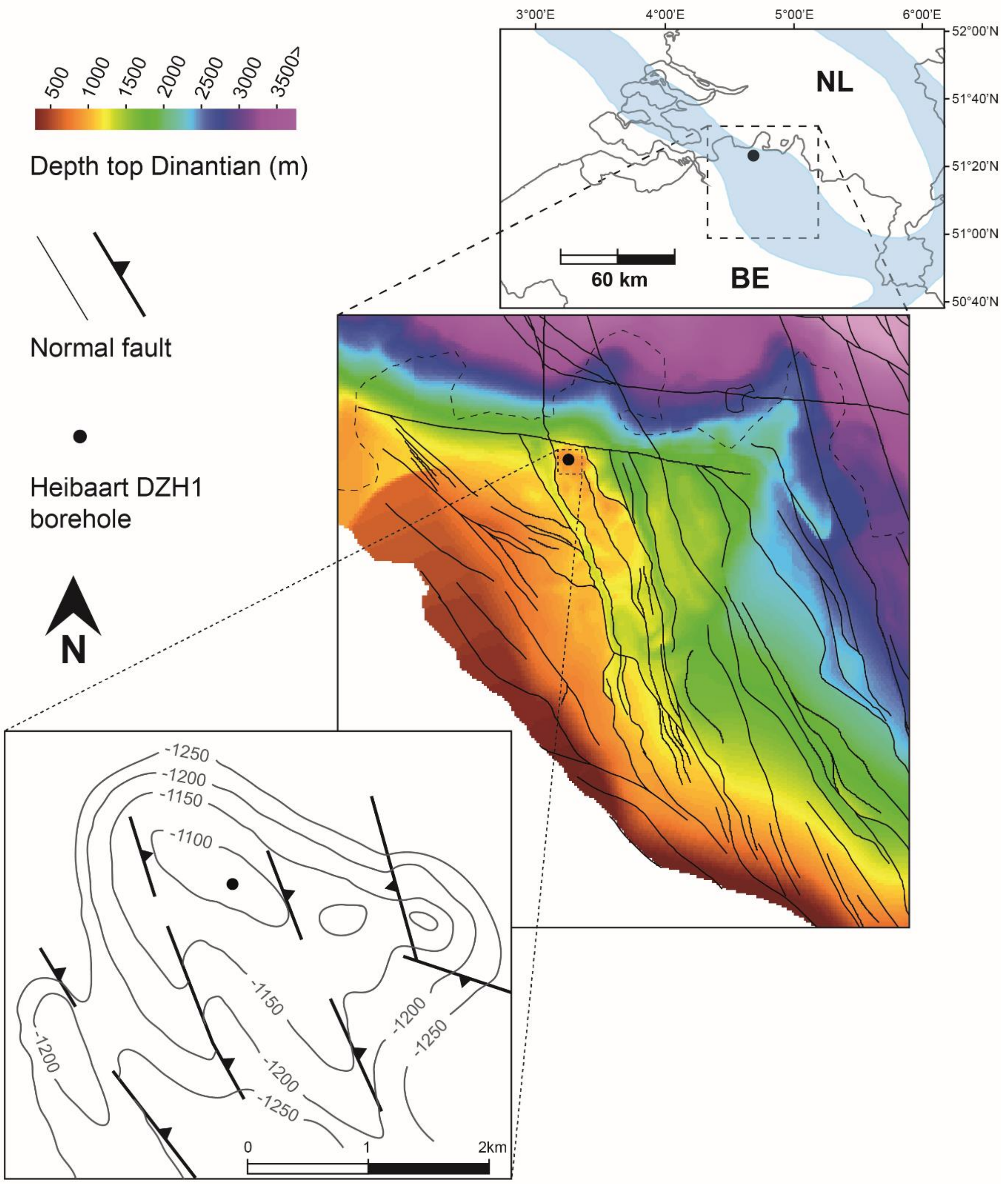

Figure 2 Structural framework around the Heibaart DZH1 borehole in northern Belgium. The map in the middle shows the regional interpretation of GEOHEAT-APP (2014). The lower left zoomed-in map is the structural interpretation presented by Bless et al. *(1981). The numbers indicate the depth of the top of the Viséan carbonates in meters below sea level.*

2.2 Sedimentology and stratigraphy

The Lower Carboniferous carbonates were deposited on a ramp or shelf (Reijmer *et al.*, 2017) and are now located at varying depths in the Campine-Brabant Basin.

Paproth *et al.* (1983) made a first overview of the Lower Carboniferous lithostratigraphy in the Belgian Campine-Brabant Basin. An update was presented by Laenen (2003). Figure 3 summarizes the lithostratigraphy of the Campine-Brabant Basin in Belgium and the Netherlands. The Bosscheveld Formation forms the transition from Devonian siliciclastic deposits to the Lower Carboniferous 'Kolenkalk Group' and consists of an alternation of sandstones, siltstones, claystones and limestones. It is only found in the southeastern part of the Campine-Brabant Basin. The overlying dark claystones of the Pont d'Arcole Formation are the base of the Kolenkalk Group and are covered by Tournaisian to lower Moliniacian dolostones of the Vesder Formation. The massive limestones of the Steentje-Turnhout Formation overly the dolostones conformably and are covered by bioclastic wacke- to grainstones of the Velp Formation. On top of this, the Loenhout Formation consists of fossiliferous mudstones, bio- and lithoclastic wacke- to grainstones and boundstones, locally intercalated with clay-rich layers. The Kolenkalk Group is disconformably overlain by thin-bedded dark chert-bearing limestones, dolostones and claystones of the Souvré Formation (Laenen, 2003). Some other local formations were identified in the most western and eastern part of the Belgian Campine-Brabant Basin (fig. 3).

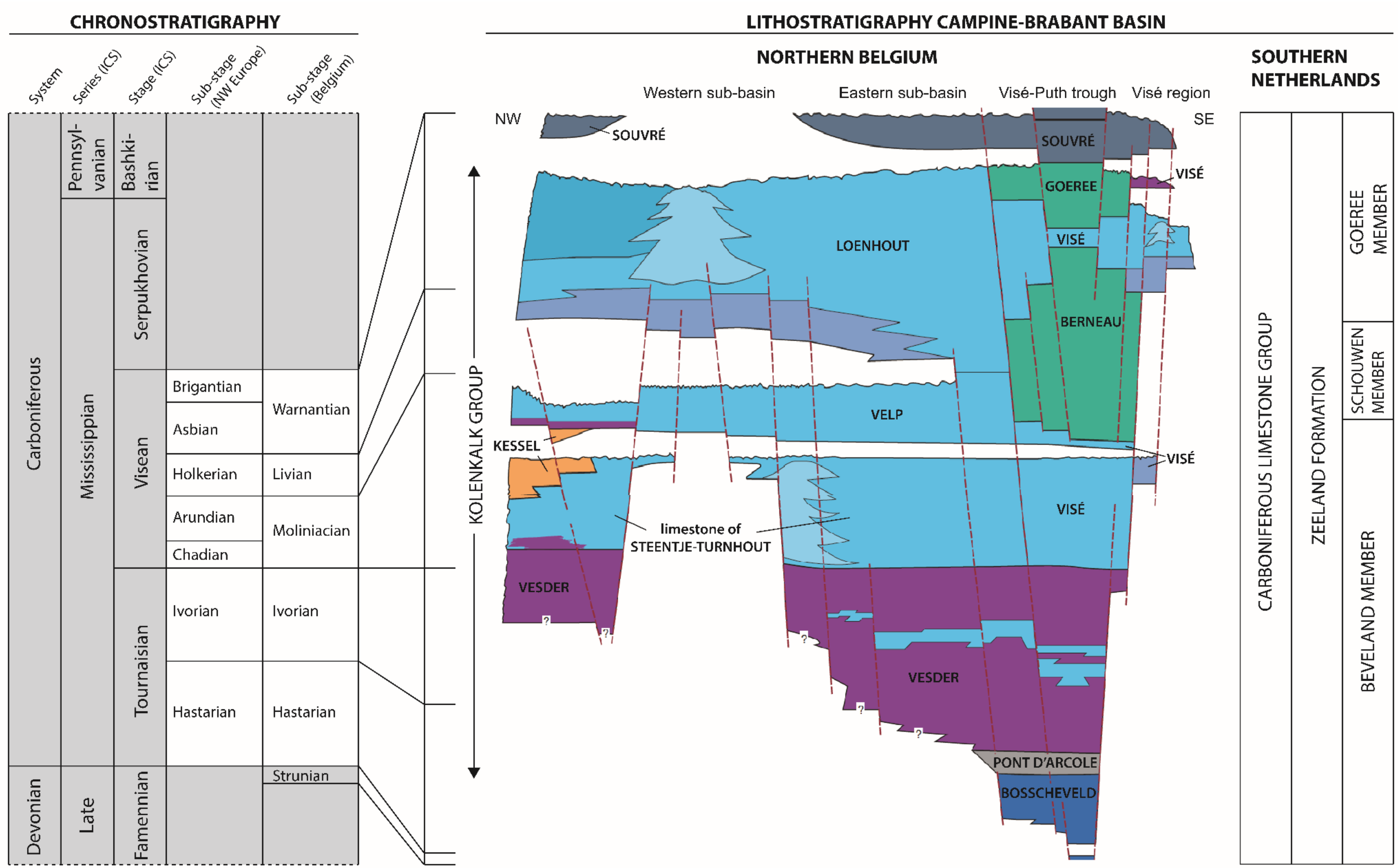

Figure 3 Chrono- and lithostratigraphic subdivision of the Lower Carboniferous carbonates in the Campine-Brabant Basin in northern Belgium (Laenen, 2003) and the southern Netherlands (Van Adrichem Boogaert & Kouwe, 1993-1997).

In the Netherlands, the Lower Carboniferous carbonates comprise one formation, i.e. the Zeeland Formation or Carboniferous Limestone Group (Van Adrichem Boogaert & Kouwe, 1993-1997). It is subdivided into three members: the Tournaisian to early Viséan Beveland Member consisting of dolostones with intercalations of limestone, siltstone and claystone, the early to late Viséan Schouwen Member characterized by fossiliferous limestones, and the late Viséan Goeree Member which contains partly silicified dark limestones.

A stratigraphical gap between the upper Viséan carbonates and lower Namurian shales was identified near the London-Brabant Massif (Graulich, 1962; Bouckaert, 1967). An angular unconformity of basal Namurian deposits onlapping onto the Viséan, especially at the flanks of the Heibaart and Poederlee highs, was identified by Dreesen *et al.* (1987). It is thought to be the result of the Sudetic orogenic movements and a global sea level fall (Bouckaert, 1967). The hiatus coincides with a paleokarst level, recognized in parts of the Campine-Brabant Basin (Vandenberghe *et al.*, 1986; Dreesen *et al.*, 1987). This karst development, caused by the step-wise sea level fall, is most pronounced at the local highs that became exhumed. For instance in the area of the Heibaart and Poederlee highs, the karstification incised up to 200m into the underlying rocks, according to Dusar *et al*. (2015). In Heibaart, these karstified limestones are used as a reservoir for gas storage by Fluxys since 1981. Dreesen *et al.* (1987) identified different collapse structures on seismic data from the Campine Basin, most likely resulting from the dissolution of underlying carbonates. In their paleokarst model, the karstification affecting the uppermost Viséan limestones, was also guided by infiltration of meteoric water along faults and joints, causing dissolution with the development of collapse structures at deeper levels as well. During the early Namurian, the karst topography had been drowned as the result of a major transgression (Bouckaert, 1967). Even after this drowning, dissolution of carbonates continued as a result of groundwater circulation during the Namurian, resulting in additional collapse breccias (Dreesen *et al.*, 1987). A possible additional period of paleo-karstification can be linked to the uplift during the Cretaceous. Whether hypogenic karstification also affected the Lower Carboniferous carbonates in the Campine-Brabant Basin is matter of debate.

2.3 Heibaart DZH1 borehole (case study)

The Lower Carboniferous carbonates of the Campine-Brabant Basin have been subject of interest for hydrocarbon production and storage, CO_2 sequestration, and as a reservoir for deep geothermal energy. In the early eighties, exploration wells for geothermal energy were drilled in Meer and Merksplas (fig. 1; Vandenberghe, 1984; Vandenberghe *et al.*, 2000). Much later, between 2012 and 2016, five geothermal wells were drilled into the Lower Carboniferous for agricultural purposes in Californië (Horst aan de Maas), in the eastern part of the Netherlands (CAL-GT wells; fig. 1). In 2016, a geothermal doublet of the Balmatt project of VITO was finished in Mol-Donk, northern Belgium (Bos & Laenen, 2017; MOL-GT wells; fig. 1). These projects have increased the interest in the Lower Carboniferous carbonates as a deep geothermal reservoir.

In order to better understand the Lower Carboniferous carbonate reservoir characteristics and predictability in this region, wells were used to study the fracturing of the rocks from cores and geophysical well logs. The results of the studied well Heibaart DZH1 (Geological Survey of Belgium reference 007E196), located in northern Belgium, will be presented here. This borehole was drilled in 1977 by Distrigaz (Fluxys now) to explore the potential of the Lower Carboniferous carbonate reservoir for hydrocarbon storage.

Muchez *et al.* (1987) and Muchez (1988) already performed a detailed study on the sedimentology, biostratigraphy and geochemistry of the Lower Carboniferous sequence (fig. 4). Viséan carbonates in the Heibaart DZH1 borehole were intersected between 1102m and 1399m depth and are of late Moliniacian to early Warnantian age (Muchez *et al.*, 1987). The lower part (upper Moliniacian to lower part of lower Warnantian), comprises of bioclastic wacke- to grainstones interpreted to be deposited in a mostly open marine environment around normal wave base (lithotype units C, D and E; fig. 4). This well is different from most other wells in the Campine-Brabant Basin, since the upper part of the sequence (upper part of the lower Warnantian) consists of cryptalgal boundstones and laminated stromatolites which indicate that an algal-cryptalgal buildup developed in this area (Muchez *et al.*, 1987). The lower part of this buildup was deposited in an open marine environment below wave base, after a sea-level rise and deepening of the sedimentary environment (unit A). The overlying limestones with large amounts of crinoids and brachiopods (unit B) points at increased wave activity and the top part of the sequence (unit A) is interpreted to be deposited in an intertidal to shallow subtidal environment because of the cryptalgal laminites and hemispheroidal stromatolites. The 'shallowing upward' character of the buildup sequence is caused by a regression at the end of the early Warnantian and/or the growth of the buildup. The Heibaart DZH1 borehole was drilled in the top of the buildup structure. Other Viséan reefal buildup limestones were found in the boreholes of Poederlee and O18-01 (fig. 1; Muchez *et al.*, 1990; Muchez & Langenaeker, 1993; Swennen & Muchez, 1991). A similar Viséan reef mound was found in an outcrop in the area of Visé, northeastern Belgium (Muchez & Peeters, 1986). None of the other wells with Lower Carboniferous carbonates in the Campine-Brabant Basin transected Viséan buildup structures.

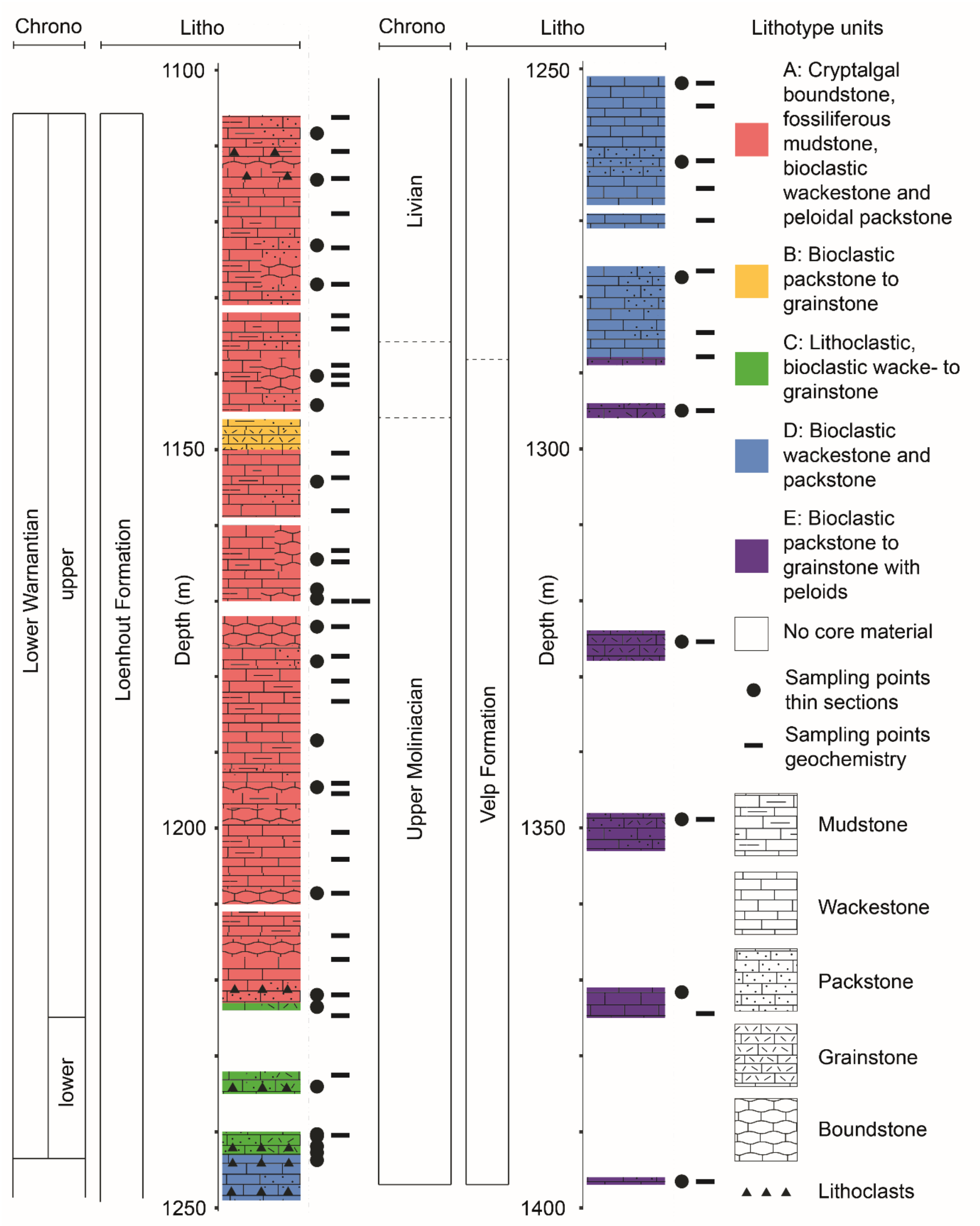

Figure 4 Chrono- and lithostratigraphic subdivision of the Viséan carbonate sequence in the Heibaart DZH1 borehole, after Muchez et al. *(1987).*

3 DATA AND METHODS

3.1 Datasets

In the case study of the Heibaart DZH1 borehole, four different datasets were used (fig. 5): 1) lithology; 2) geochemistry; 3) geophysical well logs; and 4) physical features from cores. The lithotype, geochemistry and geophysical well logs were acquired in previous work (Muchez *et al.*, 1987). The physical features from cores were newly acquired in this study. Partially open veins in the cores are the main target of interest.

In the upper 193m of the Viséan sequence, coring was performed continuously. Cores were recovered almost completely in the upper part (1102m-1224m). In the middle interval of the Viséan sequence (1224m-1295.5m), six parts of a few meters length each are missing. In the lowermost part (1295.5m-1399m), coring was performed only in four intervals of a few meters each.

The geophysical well logs, even if they date from several decades ago, reflect measurements influenced by a variety of factors, such as lithology and petrophysical properties. The influence of the partially open veins on the different geophysical well logs is also investigated in this study, since this relationship could be of great value for the prediction of permeability in fractured reservoirs.

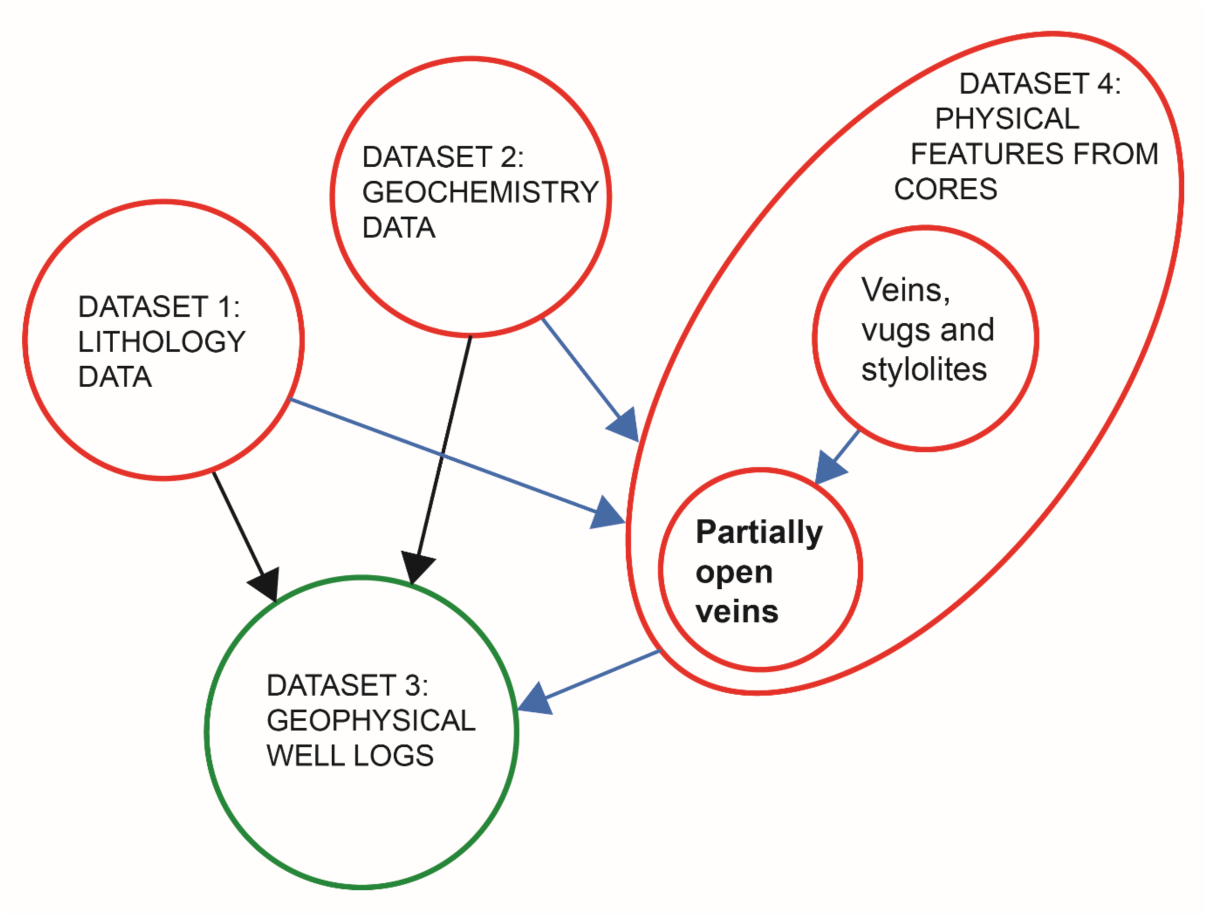

Figure 5 Overview of the datasets used. The arrows indicate which factor (possibly) influences another factor. The datasets in red circles are derived from core material. The relationships which are investigated in this study are indicated by the blue arrows, with the data on partially open veins as the most interesting target. The geophysical well logs measure the combined result of the different factors and are thus influenced by the three other datasets.

Dataset 1: lithology

As mentioned before, the lithological subdivision of Muchez *et al.* (1987) was used for the analyses (fig. 4).

Dataset 2: geochemistry

57 geochemistry measurements were available along the Viséan sequence (Muchez, 1988; Muchez & Viaene, 1990). The concentrations of the following elements were measured on bulk samples using a Varian Techtron atomic absorption spectrometer:

Mg (%), Na (ppm), Fe (ppm), Mn (ppm), Zn (ppm), K (ppm) and Sr (ppm). The standard method for the analysis of carbonates has been applied. Ca was not analyzed since it is the main element of the rock and shows almost no variation in concentration. Focus was on the other elements to study the variations. Al and Si were not measured because the minerals in which these elements are mainly present, i.e. quartz and clay minerals, do not or only to minor extent dissolve by the standard method used for carbonate analysis. After using HCl (12.5N), the percentage of insoluble residue (IR) was measured gravimetrically. The percentage of organic carbon (C), was determined by the Walkley and Black method (Muchez, 1988; Muchez & Viaene, 1990). These geochemical data were used in this study in order to examine the relationship between geochemistry, lithology and fracturing. Measurements within veins (Fe or Mn > 400ppm; Muchez, 1988) are not representative for the bulk geochemistry and were left out for further analyses. Also measurements with a higher K concentration (K > 30ppm) are left out since they do not form the scope of this study. The generally very low K concentrations could be the result of deposition on a paleo-high, which caused a very low influx of siliciclastic sediments at this location and the deposition of very pure limestones in the buildup. The remaining 46 measurements were used for further analyses (fig. 4 and appendix A).

Dataset 3: geophysical well logs

Eight different geophysical well logs were available for the Heibaart DZH1 borehole (appendix B): Thermal Neutron Porosity (NPHI), Spontaneous Potential (SP), Gamma Ray (GR), Delta-T Compressional (DTCO), Caliper (CAL), Density (RHOB), Laterolog Deep Resistivity (LLD) and Short Normal Resistivity (SN). The Viséan interval contains 6 or 7 measurements of every log per meter, to a depth of 1394m. All logs were used to investigate whether relationships exist with characteristics of joints and partially open veins.

Dataset 4: physical features from cores

The Lower Carboniferous carbonates consist mostly of shallow water limestones and dolostones that were partially fractured and karstified (Bless *et al.*, 1976; Muchez & Langenaeker, 1993). The following list of physical features and their associated characteristics were described from core material in the case study.

Veins

Veins are fractures which are cemented and thus keep the rock intact. These are easily quantifiable from cores. Although veins do not contribute to permeability, they do provide information on the mechanical nature of the rock, since they were once open fractures (Bons *et al.*, 2012). Furthermore, veins contain information on the diagenetic history of rocks. Partially open veins are fractures which are partly cemented but in which porosity is remaining. These are interesting from a reservoir perspective. Associated measurable variables are depth, width, orientation/inclination, length, aperture and open part (%).

Vugs

Vugs are non-planar cavities in rocks which are either completely cemented or partially open. They result from dissolution processes and could influence permeability in case they are connected (Barros-Galvis *et al.* 2015). For this reason, vugs were also taken into account in this study. Associated measurable variables are depth, width, height, orientation/inclination, aperture and open part (%).

Stylolites

Stylolites are pressure dissolution surfaces resulting from chemical compaction. They are often thought to act as permeability barriers or control on fluid flow as they are usually filled by clays and organic material. Generally, the presence of stylolites may decrease the permeability perpendicular to the stylolites, while the permeability parallel to the stylolites may increase (Toussaint *et al.,* 2018). Moreover, stylolites can be reactivated as fractures. Associated measurable variables are depth, width, orientation/inclination, amplitude, aperture and open part (%).

3.2 Workflow

A general workflow for the characterization of carbonate reservoir fracturing from borehole data, is presented below.

Step 1: Check of data quality, representativeness and limitations

To characterize the fracturing of a rock sequence, one would ideally acquire new data using sampling strategies and techniques designed for such a specific case. However, when dealing with an already existing dataset or a combination of different datasets, the first step is always to check the quality of the data, its representativeness and to identify possible limitations.

When dealing with a well that was drilled years or decades ago, sampling activities of previous studies and handling of the cores may have decreased the amount and coherence of the core material. In short, we can make a distinction between three different core sampling results: continuous core material, continuous core material in discontinuously cored parts, or discontinuously sampled core material. In the latter two cases, a disadvantage is that values are missing in certain parts of the studied rock sequence and it is sometimes unknown whether the cored parts are representative for the entire section or biased by rock characteristics. Also, it might be difficult to study relations between certain characteristics and lithology transitions, for instance. The borehole of the case study was continuously cored in discontinuous parts. Geophysical well logs were available for the intervals without cores.

If an already existing dataset is used for a new study, the data are often limited. In the example of the Heibaart DZH1 case study, the geochemical dataset is relatively limited in number of measurements. Furthermore, the available data did not allow to deduce information on joint distribution. Another example of a data limitation is the absence of core orientation information. Although orientations of features cannot be taken into account, the inclination of the features also contains information of the structure of the reservoir. Identifying the limitations of datasets is necessary before using them.

Step 2: Quantification of features and their characteristics from cores

Fractures are planar or subplanar discontinuities that are (very) narrow in one dimension compared to the other two and form as a result of external or internal stress (Fossen, 2010). Joints, opening-mode fractures which are completely open and not cemented, are most interesting from a reservoir perspective. As mentioned, the frequency of natural joints cannot be quantified directly from cores, since the boundary between core samples could also be the result of drilling induced fracturing or research activities in case of a previously studied core. This is also the reason why no Rock Quality Designation (RQD) log (Priest & Hudson, 1976; Deere & Deere, 1988) was used, which is the percentage of core samples longer than 10cm, often used as an indirect estimate of fracturing degree.

Macroscopic fracture quantification from (almost) continuous core material has been performed before. Laubach *et al.* (2009) present studies of sandstone and chalk cores of which fracture numbers are derived, although their quantification method was not described in detail. Sagi *et al.* (2013) used image analysis on slabbed chalk cores for fracture density quantification and “rubble size measurements” of incohesive parts for fracture density estimation.

After the description of all features and their characteristics, frequencies of the features can be quantified by dividing the number of features by the core length of that interval. After testing different interval lengths, which did not influence the results considerably, intervals of one meter were used.

Artefacts occur when measuring the length/height of certain features. Most fractures and stylolites are bounded by the walls of the borehole which results in an underestimation of the length/height. Therefore, these ‘censored’ features should not be taken into account when analyzing the length/height distribution. Almost all features in the present study are censored, since the core is 5.08cm wide. For this reason, we decided not to take into account the length/height of these features as a variable.

Step 3: Data exploration and statistical tests

A first step in the data exploration is the transformation of the variables. For most variables, the values cannot be negative. These variables with “restricted” values need a log transformation to eliminate the non-negativity problem, prior to performing statistical tests. The zero-values need to be replaced by a chosen constant (for instance 1) by adding the constant to all values before log transformation. Variables with values restricted by zero and a positive value (for instance the inclination of a feature from 0 to 90 degrees) need the following transformation:

$$T\ (x) = log\left(\frac{x_i+c}{b-x_i+c}\right)$$

in which x is the original variable, b is the positive restriction value, c is a chosen constant to eliminate 0 values, and T is the transformed variable.

Compositional data, such as the geochemical dataset in this study, need a centered log-ratio (CLR) transformation before applying statistical tests (Aitchison, 1986; Weltje, 2012; Verhaegen *et al.*, 2018). The concentrations of the different elements are dependent on each other since the sum of them is constant (100%). A CLR transformation eliminates this interdependency of the data. Each component of the data matrix is transformed by subtracting the average of the natural logarithms of all values on that row, from the natural logarithm of the original value of that component.

The transformed variables are used for all following statistical tests. We have chosen for a stepwise approach including Kruskal-Wallis and Wilcoxon tests, Spearman correlation tests and Principal Component Analyses (PCA). After performing the tests, the results can be transformed back without losing information.

Categorical versus numerical data

We tested whether differences exist between the lithotype categories for each numerical variable, such as vein frequency. In case that the variable is not normally distributed (which is mostly the case for fracture data), a non-parametric Kruskal-Wallis test will test whether differences exist between the categories or that the 'populations' are not significantly different (Davis, 2002). Subsequently, a pairwise Wilcoxon test is needed to identify which categories are different from each other.

Correlation between numerical variables

The third step is to pairwise analyze whether correlations exist between numerical variables. A linear regression can be performed for normally distributed variables, otherwise a Spearman rank correlation test is a useful alternative (Davis, 2002). In order to compare all variables to each other, the values should be averaged over a certain interval, for instance per meter.

Principal Component Analysis (PCA)

The relationships between all numerical variables can be explored using a PCA (Davis, 2002). This is a statistical multivariate procedure that reduces the dimensionality of the data in order to explain the variance of the variables.

When working with frequency variables, average values of intervals are necessary for the analyses (number per meter). This implies that some feature characteristic variables contain missing values. For instance, intervals without stylolites do not contain an average value of the stylolite amplitude. Variables with missing values cannot be taken into account in a PCA.

4 RESULTS

4.1 Physical features from cores

Figure 6 shows examples of all physical features which were described and measured from the cores: veins, partially open veins, cemented vugs, partially open vugs and stylolites.

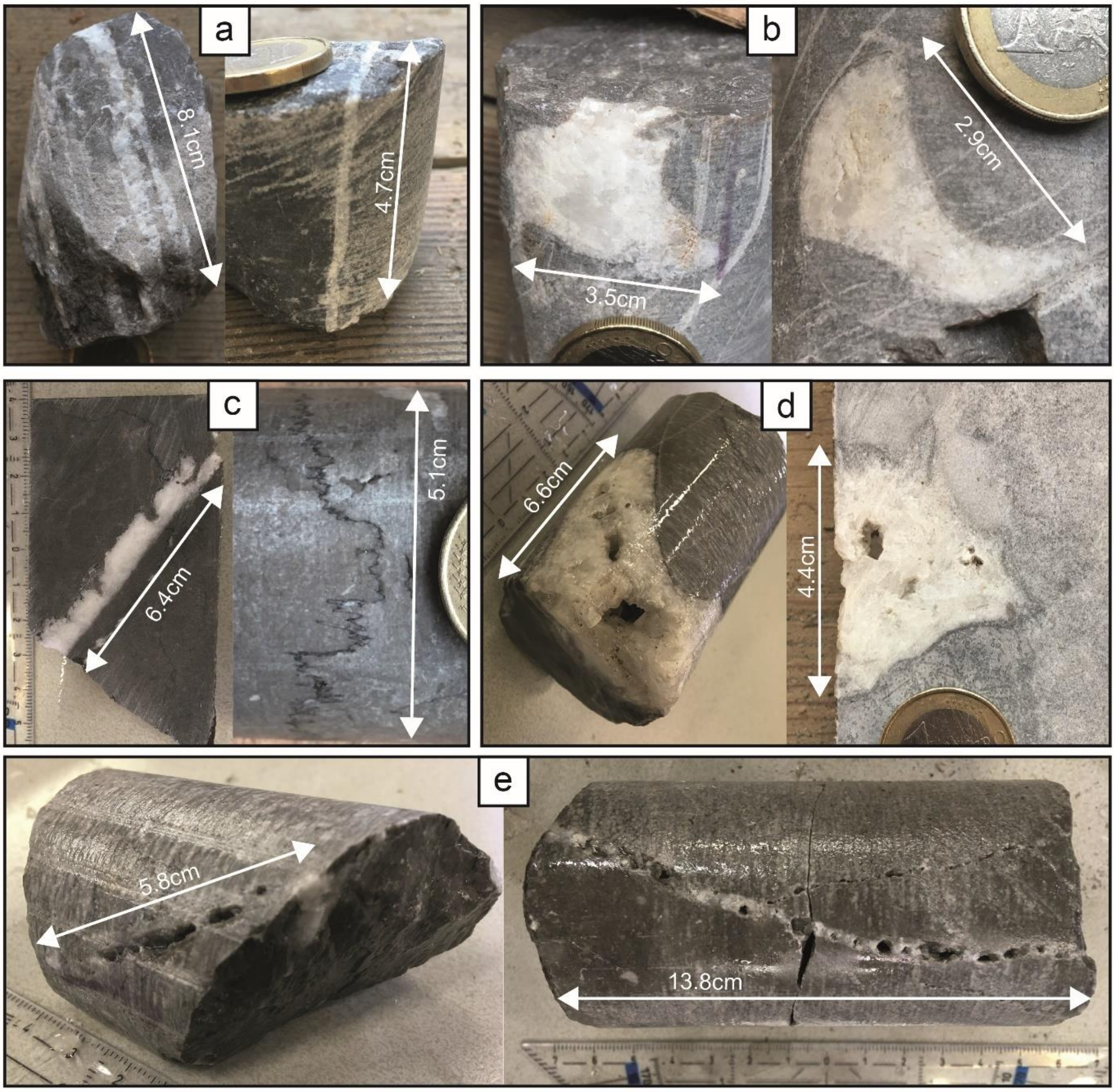

Figure 6 Examples of core samples from the Heibaart DZH1 borehole with (a) veins at 1124.0m (left) and 1246.9m (right), (b) cemented vugs at 1212.5m and 1202.5m, (c) stylolites at 1251.3m and 1215.5m, (d) partially open vugs at 1155.0m and 1137.8m and (e) partially open veins at 1178.0m and 1284.7m.

In figure 7, the frequencies of veins, partially open veins, stylolites, cemented vugs and partially open vugs are plotted along the depth of the borehole. The veins (which are all opening-mode fractures and completely cemented) are most abundant in the upper 110m of the sequence and around 1263m and 1288m (see grey highlighted zones in figure 7 with a threshold of 20 veins per meter). Veins are clearly least abundant in the interval between 1220 and 1245m (roughly lithotype unit C; fig. 2). Most partially open veins exist in the upper 100m, with a major peak around 1180m depth and minor peaks around 1135m, 1163m and 1280m. Even in the lowermost part of the sequence, open veins were found around 1396m. The stylolite frequency shows a large variation with a main peak around 1203m. Stylolites are also abundant between 1265m and 1288m (lower part of lithotype unit D). Cemented vugs are abundant in the upper 140m of the sequence (peaks around 1117m, 1182m and 1200m) and very rare in the rest of the sequence. Partially open vugs only occur in the upper 100m, with peaks around 1119m, 1134m and 1197m.

Figure 8 shows the characteristics of the (partially open) veins, stylolites and (partially open) vugs with depth. For veins at the edge of a sample, the minimum width was used. Two intervals with pure calcite pieces were found (104cm at 1140.11m and 13cm at 1167.14m), which resemble veins with a width larger than the core diameter (>5.08cm). Since the inclination is not exactly clear, the real width is not known and the minimum width was taken into account. The veins are mostly 0.1 to 5mm wide, but wider veins occur, mostly in the upper 100m of the sequence. The width of partially open veins varies more and is largest around 1125m depth. The inclination of veins and partially open veins is most often between 70 and 90 degrees from horizontal (largest data point density in figure 8). Since the borehole was drilled vertically, the chance of drilling through sub-vertical fractures is lower than through horizontal fractures. Therefore, the fact that most observed fractures have an inclination between 70 and 90 degrees means that sub-vertical fractures are clearly dominant in the Viséan carbonates at this location. However, there is a larger variation of the inclination of veins, especially in the upper 150m. The inclination of stylolites varies even more, although an inclination between 0 and 30 degrees seems most abundant. The aperture of partially open veins is largest between 1118m and 1140m, and around 1186m, where this type of veins is most frequent, with one additional large aperture at 1371m. The open part of these veins exceeds 40% at 1147m, between 1173m and 1211m, and around 1280m. Stylolite amplitudes are largest between 1264m and 1288m, where stylolite frequencies are also relatively high. The aperture and open part of partially open vugs are rather variable and correspond to only 26 measured vugs.

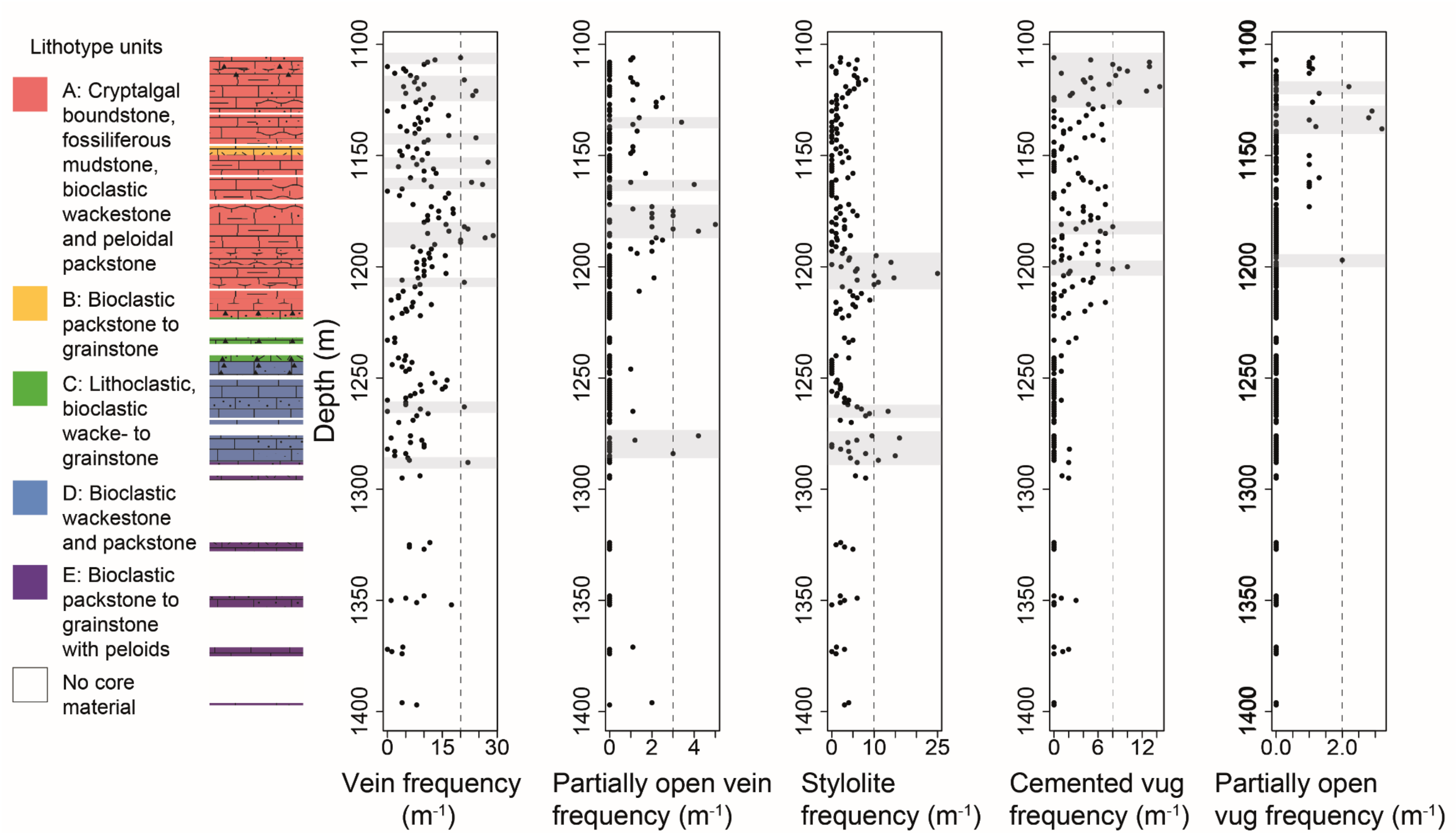

Figure 7 Frequency of veins, partially open veins, stylolites, cemented vugs and partially open vugs, observed in the core material, along the depth of the borehole. Zones in which values exceed a chosen threshold (dashed line) are highlighted in grey to emphasize variations. The cored intervals and lithotype subdivision (fig. 2; Muchez et al., *1987) are shown on the left.*

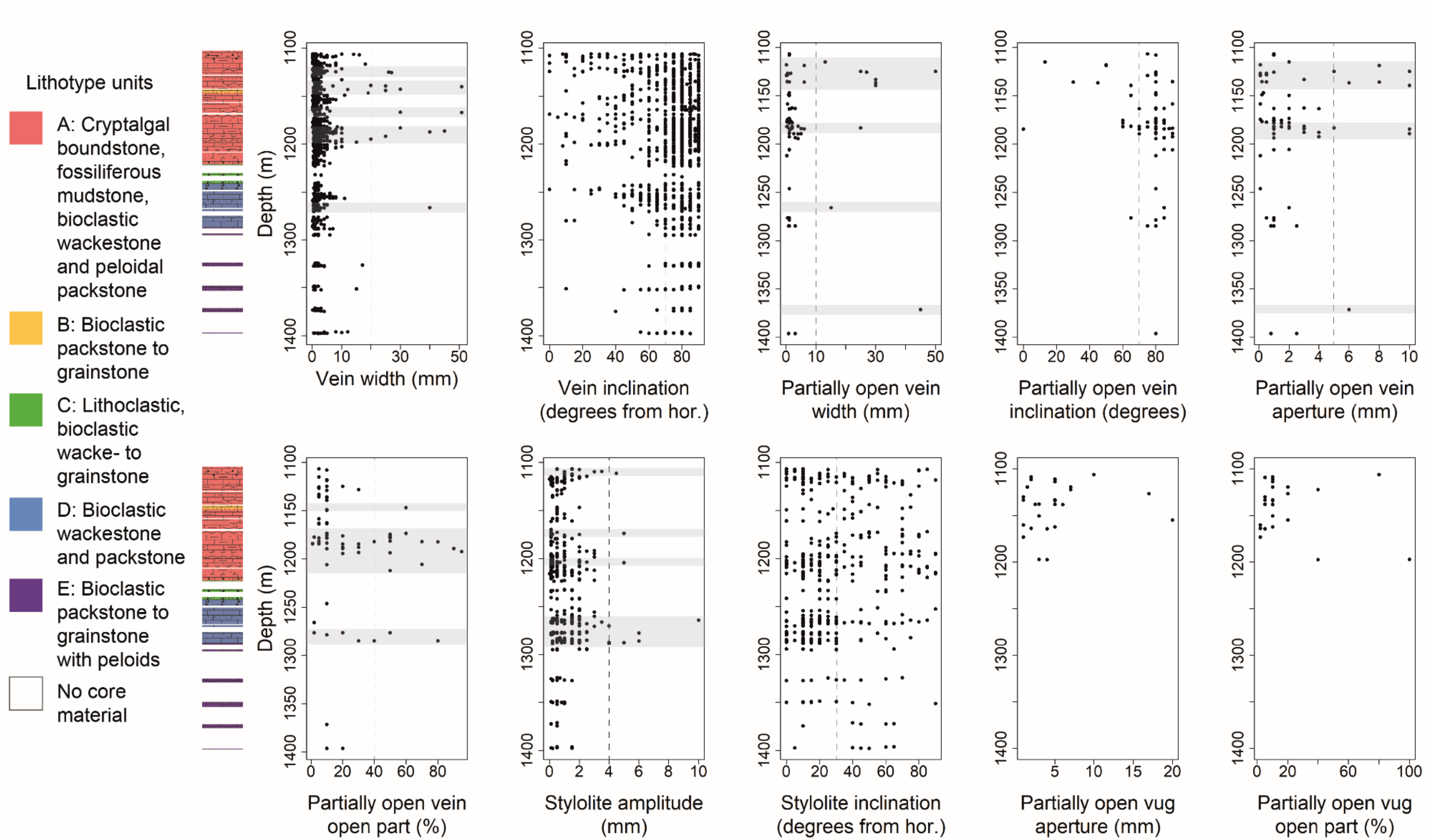

Figure 8 Characteristics of physical features observed in the cores, along the depth of the borehole. Zones in which values exceed a chosen threshold (dashed line) are highlighted in grey to emphasize variations. The cored intervals and lithotype subdivision (fig. 2; Muchez et al., *1987) are shown on the left.*

4.2 Kruskal-Wallis and Wilcoxon tests

Kruskal-Wallis tests were performed, with a confidence level of 95%. For some variables, no significant differences between lithotype units were found. Subsequently, a pairwise Wilcoxon test was done for the transformed variables of which the values differ significantly among the lithotype units, to check which lithotype units differ significantly from each other and in which order (appendix C).

Partially open vugs were only found in unit A, and also the variables of the frequencies of veins and cemented vugs were largest in this unit. The variables of NPHI, CAL, RHOB, LLD and SN logs are relatively high in unit A, while the GR variable shows low values. Unit A has relatively low C and K values and relatively high Fe values.

Since unit B is a small interval, the number of measurements in this interval are also limited, and there are no geochemistry measurements of unit B. The studied variables are mostly close to average in this unit. However, the tests show that the SP variable contains the lowest values, compared to the other units.

Lithotype unit C also contains quite average values of most variables. However, the vein frequency variable is lowest in this unit and the two resistivity variables contain relatively high values. Small peaks in the K and Mg values are present around the boundary between unit A and C. Unit C contains the highest values of these elements, although only 3 measurements are available in this unit and the results were not statistically different from the other units.

The veins and stylolites in unit D are more horizontal than in other units (fig. 8 and Appendix C). The variables of the stylolite amplitudes and the SP log are larger, while the values of the DTCO variable are relatively low. The Fe values in unit D are lower than in other units.

In unit E, the K and GR variables show relatively high values. The DTCO variable of unit E contains higher values than the other units, while the CAL and the two resistivity variables contain lower values than the other units.

4.3 Principal Component Analyses (PCA)

A principal component analysis was performed for the geochemistry, geophysical well logs and physical features separately. Apart from these, a categorical lithotype dataset exists, for which no PCA could be performed.

Dataset 2: geochemistry

The PCA results of the transformed geochemical variables are shown in figure 9. This figure shows the individual data points (dots) as well as the variables (vectors) in the CLR space defined by the two main principal components. The two main principal components explain 56.0% of the variability of the data. Variables which plot parallel and in the same direction are positively correlated, variables which plot parallel but in the opposite direction are negatively correlated and perpendicular variables are not correlated. Figure 9 shows that the CLR scores of Na and Sr are positively correlated. Another positive correlation is visible between K and C, although the vector of C is much smaller than the vector of K. This means that the CLR score of C has a small effect on the two main principal components, and that the effect of C is largest on another principal component, in this case the fourth. The Mg and IR CLR scores are clearly negatively correlated. The CLR scores of Fe and Mn are roughly negatively correlated to those of K and C.

The first principal component is influenced mainly by the concentrations of K, IR, Mn, Mg and Fe. The second principal component is mostly influenced by Sr, Zn and Na and in a lower degree by Mg. CLR scores of C are dominant in the fourth principal component.

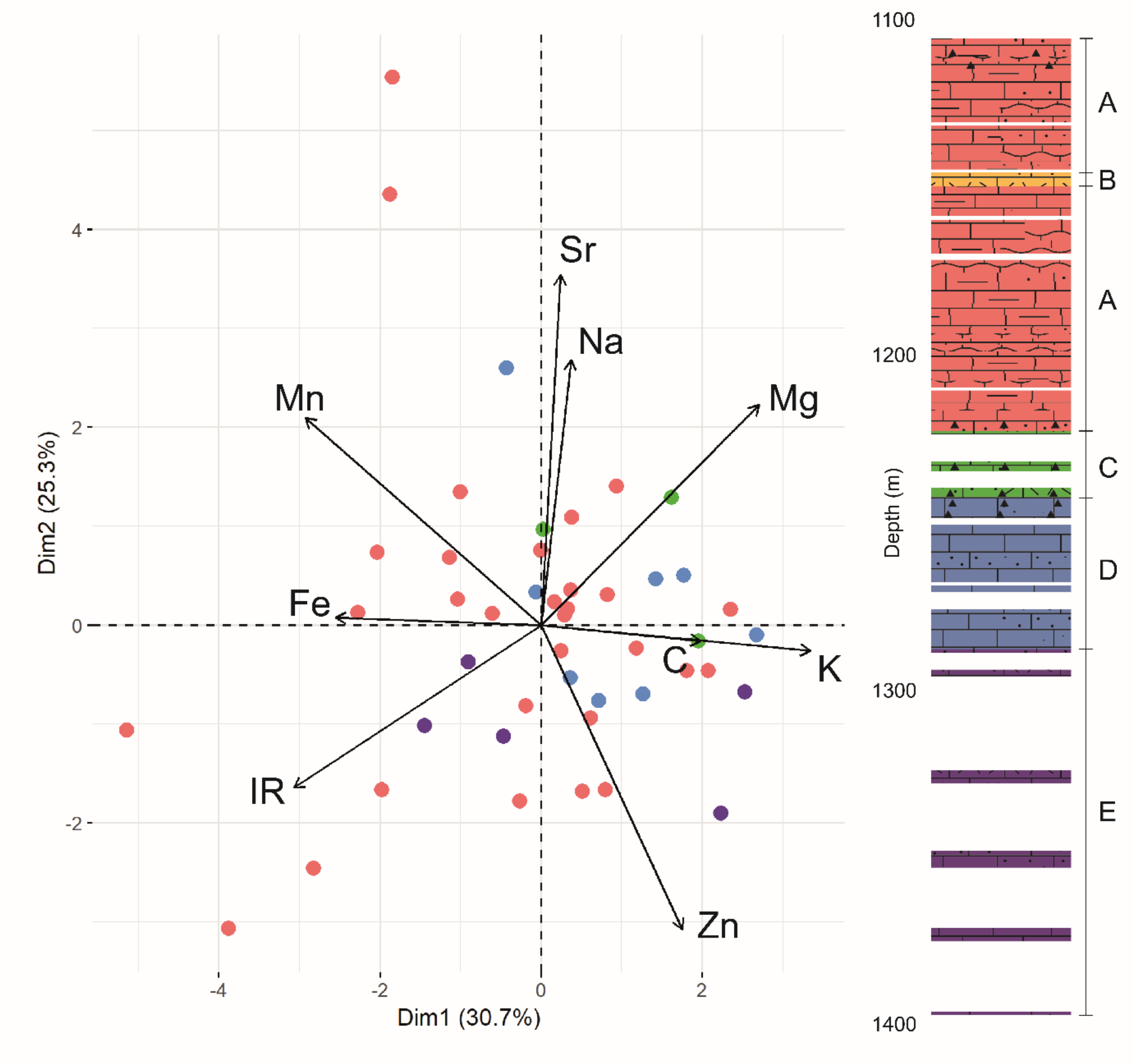

Figure 9 PCA biplot of the CLR transformed geochemistry data of the Heibaart DZH1 borehole. The x-axis represents the first principal component, which explains the largest part of the variability in the data, i.e. 30.7%. The y-axis represents the second principal component, which explains 25.3% of the variability. The dots show the individual data points within this frame. The colors of the points correspond to the lithotype units, illustrated along the borehole depth on the right (no geochemistry data were available for unit B). The vectors show the variables, in this case the CLR scores of the element concentrations.

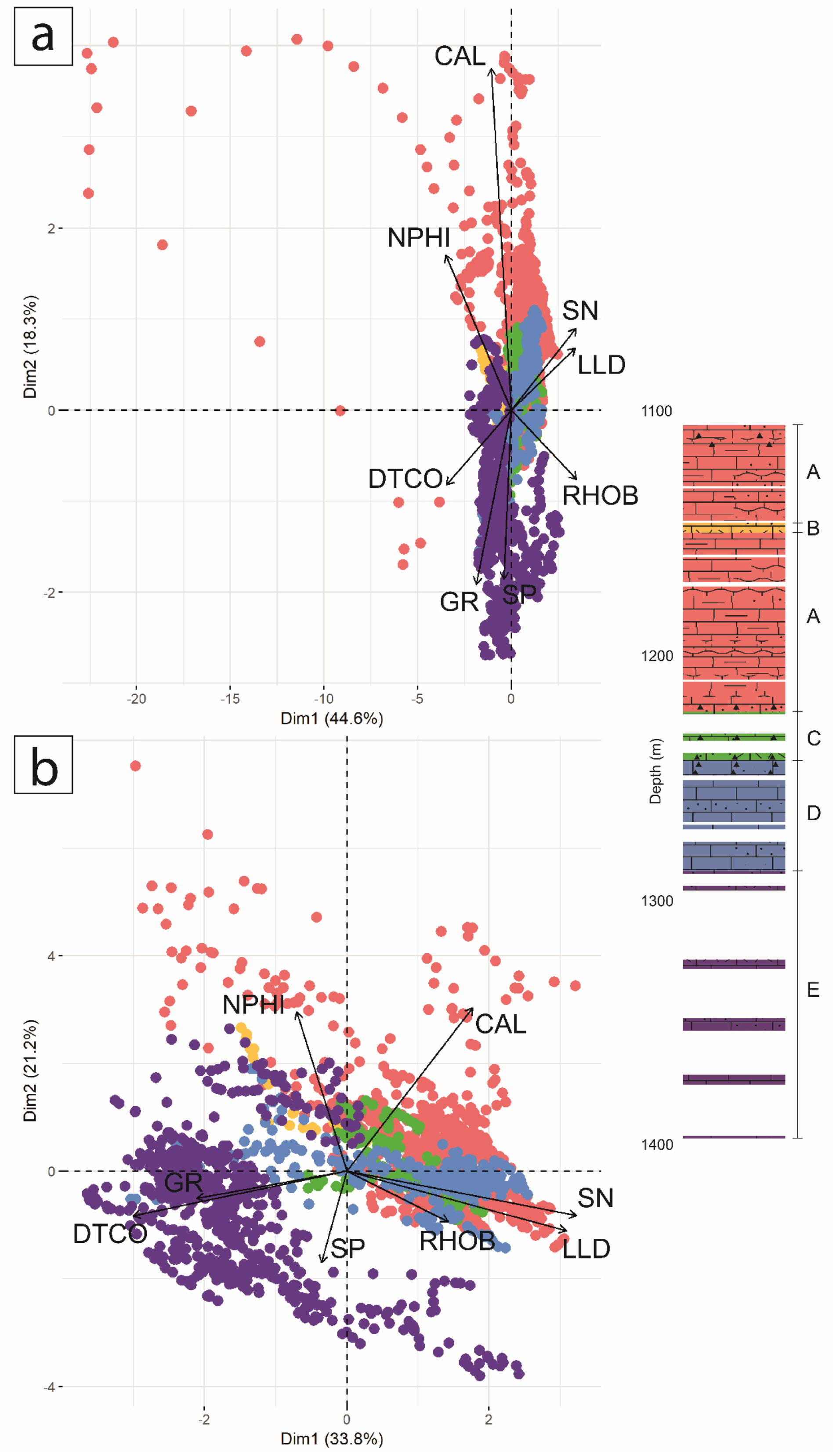

Figure 10 PCA biplot of the transformed geophysical well log variables of the Heibaart DZH1 borehole (a). 26 outliers which largely influenced the results were not taken into account in (b), in order to emphasize the maximum variation.

Dataset 3: geophysical well logs

When performing a PCA on the transformed data of the geophysical well logs, only 26 of the 1843 data points contribute together 69.8% to the first principal component and 7.2% to the second principal component. This means that these 26 points have such extreme values that they explain the largest part of the variability and thus greatly influence the results (fig. 10a). These measurements are from the sequence between 1126m and 1130m depth and are most likely the result of a lithology that is completely different compared to the rest of the section, possibly as a result of ghost-rock karstification (cf. Dubois *et al.*, 2014). The latter is a two-stage process of in-situ weathering of carbonates in which chemical dissolution is the first step. Soluble particles are removed and a ghost-rock feature is formed, which is characterized by a residual alterite often containing a lower density, higher porosity and lower $CaCO_3$ content than the original rock. The physical appearance of the resulting rock is similar to the original rock, although it has been altered. It differs from 'karstification by total removal' since open galleries only form if subsequent mechanical erosion of the undissolved particles occurs, which requires high hydrodynamic energy. Ghost-rock features in Lower Carboniferous carbonate outcrops in southern Belgium were described by Dubois *et al.* (2014).

In order to study the real interdependencies between the different log variables, these 26 outliers were left out from the PCA (fig. 10b). The two main principal components explain 55.0% of the variability. The first principal component is positively influenced by the deep and shallow resistivity variables, and negatively by the DTCO variable. The second principal component is mainly influenced by the CAL and NPHI variables. The density variable dominates the third principal component, and the SP variable the fourth. Unlike the PCA results of the geochemistry (fig. 9), the data points of the different lithotypes are clearly grouped in figure 10, instead of randomly distributed. It also shows the general values of the logs for the different lithotype units. For instance, unit E contains relatively high DTCO and GR values, while unit A contains higher NPHI and CAL values.

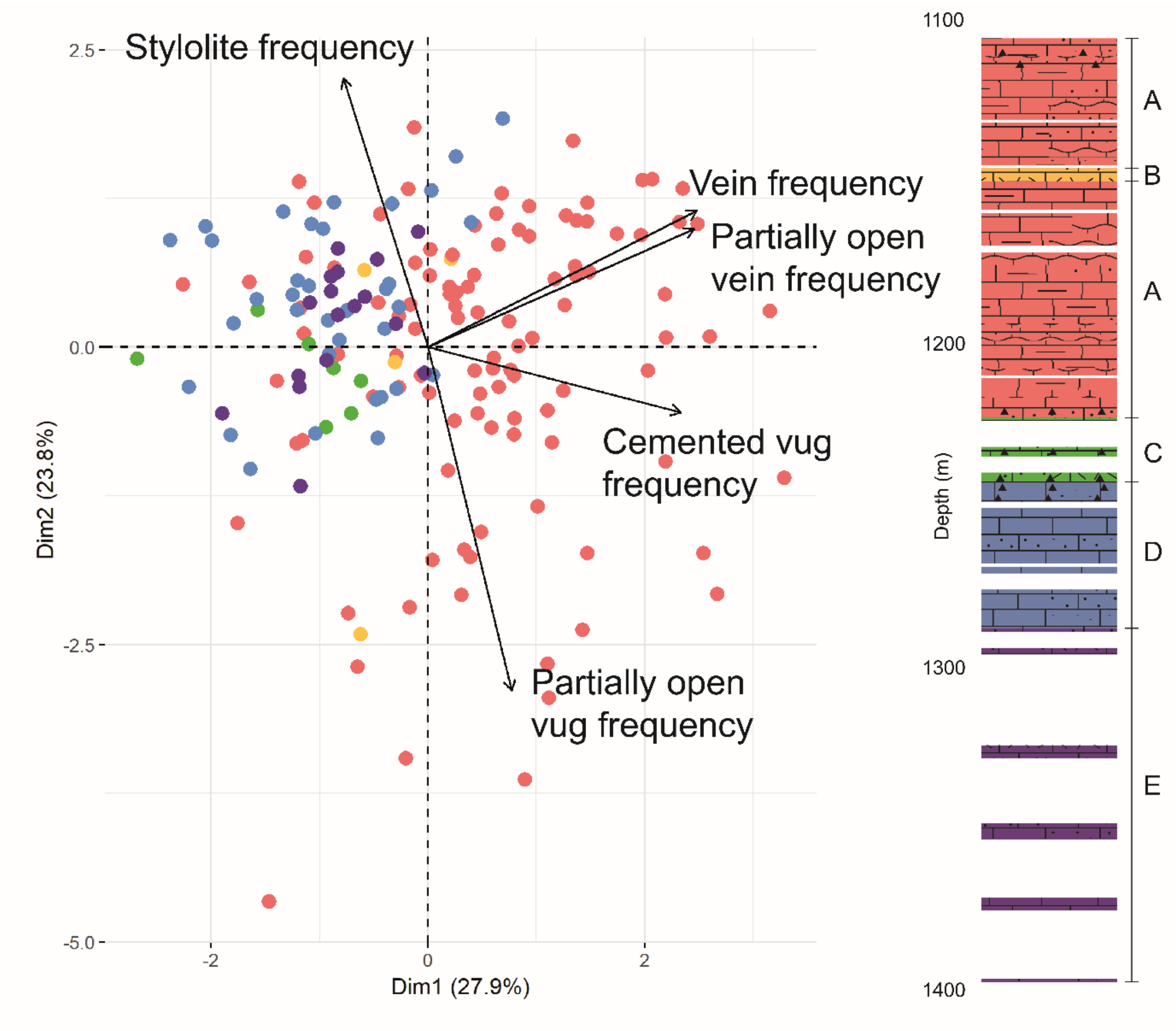

Figure 11 PCA biplot of the log transformed feature frequency data of the Heibaart DZH1 borehole.

Dataset 4: physical features from cores

The PCA results of the transformed feature frequencies are shown in figure 11. The variables of vein frequency and partially open vein frequency are positively correlated. These are perpendicular and thus uncorrelated to the variables of stylolite frequency and partially open vug frequency, which are negatively correlated to each other. The first principal component is mainly influenced by the variables of vein frequency, partially open vein frequency and cemented vug frequency. The second principal component is mainly affected by the variables of partially open vug frequency and stylolite frequency. The two main principal components explain 51.7% of the total variability. Figure 11 shows that the variables of vein frequency, cemented vug frequency and partially open vug frequency are significantly larger in lithotype unit A than in other units. The vectors of these variables point in the direction of the data of unit A. The arrow of the partially open vein frequency also points in this direction, but there is no significant difference of this frequency between the units.

4.4 Spearman rank correlation tests

The PCA analyses have shown the existing correlations between variables within the same dataset. In order to compare variables from different datasets, Spearman rank correlation tests were performed on the averaged data per meter interval. Since the feature characteristic variables contain missing values in different intervals, these could not be compared to each other by a PCA and were thus incorporated in the Spearman tests. In case two variables are both a characteristic of the same feature (for instance stylolite amplitude and inclination), the test was performed on the original data instead of the average values per meter interval. In appendix D, the significant results of these Spearman rank correlation tests are presented, using a confidence level of 95%. The correlations were checked using cross-plots of the variables. In some cases, a result with a large correlation coefficient (rho value) appeared to be based on a rather small number of data points and therefore, no major conclusions can be drawn from it. This is the case for most correlations between feature characteristic variables and geochemistry variables, since these variables both contain large percentages of missing values in the meter intervals (appendix E). The most important results are summarized below.

Significant positive correlations exist between variables of stylolite frequency, K concentration and SP log values. The SP variable is also positively correlated to the amplitude and negatively to the inclination of stylolites.

The frequency variables of veins, partially open veins and cemented vugs are positively correlated to each other. Also, wider veins contain wider but shorter open parts, while thinner veins contain thinner but longer open parts. The vein frequency variable is positively correlated to the vein width variable.

The frequency variables of veins, partially open veins and partially open vugs are negatively correlated to the K variable. The vein frequency variable and Mg are also negatively correlated. Also, a significant positive correlation exists between the variables of vein width and Mn.

The DTCO log, NPHI log and RHOB log contain so few variations that no clear correlations can be inferred with other variables. The vein frequency variable is negatively correlated to the SP variable. Significant positive correlations exists between the open part of partially open veins and the two resistivity variables. Also, the aperture is positively correlated to the short normal resistivity variable. Additionally, significant correlations exist between the resistivity variables and variables of vein frequency, width and inclination. The correlations between the vein width variable and the resistivity variables are strongest.

Significant positive correlations exist between the IR variable and the resistivity variables. A significant positive correlation exists between the GR and K variables, and a negative correlation between the GR and IR variables.

5 INTERPRETATIONS AND DISCUSSION

The aim of this study was to assess which factors control the distribution and characteristics of (partially open) fractures, and to which extent. In this context, interpretations and explanations are discussed below.

5.1 Differential compaction

5.1.1 Carbonate lithotype strength

The open fractures, which include joints and partially open veins, are the most interesting features from a reservoir perspective, since these may enhance permeability. Both are initially formed by mechanical fracturing (Bons *et al.*, 2012), after which they remained (partially) open or were re-opened later.

In order to investigate which lithotypes were more intensely fractured and which less, we studied both cemented veins and partially open veins. Veins do not contribute to permeability, but are the relicts of rock fracturing in the past. The distribution of veins, partially open veins together, provides essential information about which factors affect the formation of fractures.

Lithotype unit A, which contains cryptalgal boundstones, has the highest vein frequency. The lowest vein frequency is present in lithotype unit C, consisting of wacke- to grainstones. Alzayer (2018) found that the uniaxial compressive strength (UCS) of boundstones is generally higher than that of other carbonate lithotypes, such as wackestones, packstones and grainstones. During burial, the wacke- to grainstones of unit C could accommodate a larger amount of pre-failure strain by mechanical compaction, while early fractures developed in the stronger boundstones of unit A. The higher vein frequency observed in unit A could point to the differential compaction mechanism described by Alzayer (2018).

5.1.2 Layer-parallel slip (LPS)

The nature of bedding planes controls fracture intensity (Cooke *et al.*, 1999; Sanz *et al.*, 2008; Smart *et al.*, 2009; Alzayer, 2018). Some bedding contacts favor layer-parallel slip (LPS), while others are resistant to such slip. Alzayer (2018) demonstrated that fracture intensity is higher in the latter situation. The LPS could dissipate some of the stress, while in limestones resistant to LPS all strain is accommodated by the development of fractures.

Unit A contains a very low potassium concentration, high resistivity, low gamma ray values and high density, which indicates that it consists of very pure limestones. The latter is rather logical knowing the depositional setting of these mound carbonates, i.e. they formed by in situ growth and not by sediment deposition.

In lithotype unit C, the K and Mg concentrations are relatively high. The potassium is likely present in clay minerals. Most clays in the Viséan limestones in and around the Campine-Brabant Basin are illitic (Thorez & Bourguignon, 1973; Thorez, 1987), and hence rich in potassium. The K occurs adsorbed to the clays and in the crystal lattice. Only a small part of this K is released from the clays during the dissolution procedure applied for carbonates, explaining the low K content in the geochemical analyses. The higher Mg concentrations could be caused by more Mg-rich calcites, especially in the less recrystallized fine-grained wackestones and/or due to a slightly higher clay content. Both explanations are often related, i.e. slightly more clay in a fine-grained limestone, which formed through deposition of the particles. As is the case for K, Mg can be adsorbed or incorporated in the clay minerals and is only partly released in the analytical procedure. The slightly higher clay content is also reflected in the sonic (DTCO) and resistivity responses, which are lower in unit C than A, and the slightly higher GR log in unit A. Unit E also contains a slightly higher clay content, based on its higher K and GR variables.

Significant negative correlations exist between vein frequency variables and variables related to clay minerals. The PCA results of the geochemistry dataset (fig. 9) show that the K and Mg variables together largely influence the first principal component. To a smaller degree, also organic carbon contributes positively to the first principal component, which is not surprising since organic carbon is often enriched in more clay-rich layers and stylolites (Toussaint *et al.*, 2018). Furthermore, the vein frequency variable is positively correlated to the density and resistivity variables, which likely means that the most 'pure' limestones were fractured more intensely than the slightly less 'pure' limestones. The small amount of clay minerals which make the limestones less 'pure', are enriched in stylolites. The difference in fracturing degree is presumably related to the difference between layered limestones and non-layered, massive limestones. The limestones in lithotype unit C and E of the Heibaart DZH1 borehole likely underwent LPS, leading to a smaller degree of fracturing than the non-layered limestones of unit A.

5.2 Authigenic quartz

It is possible that silicification of the limestones has strengthened the matrix, causing a larger fracturing degree during subsequent phases because of its competence. The relatively high IR concentration in unit A could be caused by the presence of (authigenic) quartz or clay minerals. Since the GR is lowest in unit A and K values are also rather low, it is unlikely that the higher IR values are caused by clay minerals. Furthermore, the PCA results (fig. 9) show that both the K variable (associated with clay minerals), as well as the Mg variable (associated with Mg-rich calcites and clay minerals), affect the first principal component positively, while the IR variable has an opposite effect. It is highly likely that the high IR values result from authigenic quartz crystals, which are abundant in unit A (Muchez *et al.*, 1987; fig. 12). No significant correlation exists between the IR variable and any feature frequency, but the partially open vein frequency peaks around 1130m and 1180m. These peaks are also visible in the concentration of IR. However, Muchez (1988) mentions that the authigenic quartz crystals are dominantly present in and around the veins. This would suggest that the fractures are older than the quartz crystals and the fractures acted as fluid pathways for element transport.

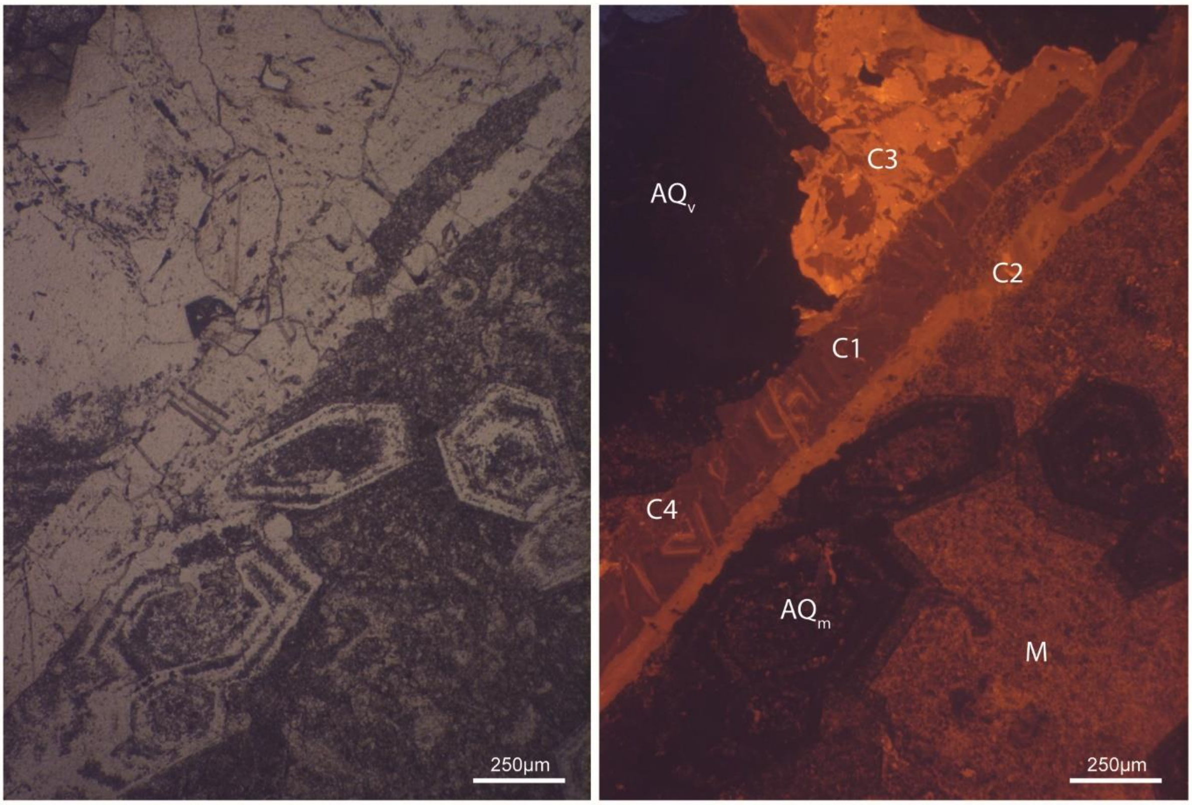

Figure 12 Transmitted light (left) and cathodoluminescence (right) images of a core sample from the Heibaart DZH1 borehole at a depth of 1191.8m. In the lower right part of the image, authigenic quartz (AQ_m) crystals in a recrystallized matrix (M) are visible. A vein is present in the upper left part, consisting of different calcite cement phases (C1-4) and authigenic quartz (AQ_v).

5.3 Partially open veins

Joints and partially open veins contribute most to permeability and are initially created by mechanical fracturing (Bons *et al.*, 2012). Consequently, some of these fractures become completely cemented, turning into veins. Partially open veins were either only partially cemented, or they were re-opened later by new fracturing or dissolution processes.

The frequency variable of partially open veins does not differ significantly between the different lithotype units. The partially open vein frequency variable is positively correlated to the frequency variables of veins and cemented vugs, as shown by the Spearman rank correlations (appendix D) and PCA results (fig. 11). This could be explained in two ways.

A first explanation is that the partially open veins were created by a later fracturation phase than the completely cemented veins, and that these new fractures developed preferentially in the intervals which already contained veins (and vugs). According to Holland & Urai (2010), the location of a next fracture after the sealing of previous ones, is dependent on the ratio between the tensile strength of vein cement, matrix and interface. If the strengths of these three elements are approximately the same, the material strength is homogeneous and a random pattern will evolve. However, if the strengths of the vein cement and the interface are smaller than the strength of the matrix, new fractures will develop in or along older veins. This could explain the correlation between the frequency variables of cemented and partially open veins.

A second possibility is that the partially open veins are older veins which were re-opened by meteoric or hydrothermal dissolution. This would explain why the partially open veins occur mainly in the intervals with high vein frequencies. Many veins in the

Heibaart DZH1 cores contain different cement phases (fig. 12), so reactivation clearly took place. It is known that karstification affected the Heibaart dome structure at the end of the Viséan (Dreesen *et al.*. 1987; Dusar *et al*., 2015). During this phase, dissolution took place and likely opened older veins.

Based on the results of this study, no compelling conclusions can be drawn regarding the development of partially open veins and the quantitative importance of both processes. Therefore, a detailed petrographical study is recommended, which is ongoing at the moment.

The open part (%) of the partially open veins is positively correlated to both resistivity variables, and the aperture variable is positively correlated to the short normal resistivity variable. These higher resistivity values could not result from the open veins, since a fracture filled with saline water, as encountered in the Lower Carboniferous limestones (Vandenberghe *et al.*, 2000; Bos & Laenen, 2017), is conductive and would lower the resistivity. It is more likely that the wider and longer vein openings are preferentially present in the most ‘pure’ limestones, which are more resistive.

6 CONCLUSIONS

A general workflow was presented for the characterization of fracturing from borehole data by extensive data analyses of different integrated datasets. In the demonstrated case study, four different datasets of the Heibaart DZH1 borehole were used to analyze the factors controlling the distribution of partially open veins and joints, which enhance the permeability of the reservoir. Although joints are most interesting, since these are by definition not cemented, the datasets acquired in the borehole did not allow to draw conclusions about the distribution of joints. However, insights were found with regard to the distribution and characteristics of partially open veins. The development of partially open veins is two-folded. In the first place, mechanical fracturing is needed, which is concluded not to occur randomly. Differential compaction controls the development of fractures. Our results show that fracturing preferentially occurred in the reefal buildup boundstones, which generally have a larger rock strength than other carbonate lithotypes. These boundstones, resulting from in situ microbial growth processes, are more competent than the layered wacke- to grainstones, which result from sediment deposition, and therefore fracture easier within similar stress conditions. Furthermore, bed boundaries in sedimentary limestones could decrease fracture development when layer-parallel slip occurs along these bedding surfaces, accommodating part of the stress. This probably occurred in lithotype unit C, consisting of lithoclastic, bioclastic wacke- to grainstones, which contains the lowest vein frequency.

Because the partially open veins are still open today, they must have remained open since the mechanical fracturing (only partially filled by cements), or they have been re-opened later after being cemented first. A positive correlation was found between the frequency variables of cemented veins and partially open veins. This could be explained either by (re-)opening due to later fracturation, or re-opening by dissolution. A combination of both is also possible.

The resistivity variables are positively correlated to the vein frequency variable, since fractures preferentially developed in the most ‘pure’ reefal buildup boundstones instead of the layered limestones with a slightly larger clay mineral content. Also, the open part (%) of the partially open veins is positively correlated to the resistivity variables. The ability of resistivity logs to predict fracture distribution should, however, be tested in other boreholes, ideally with a similar Lower Carboniferous carbonate sequence and an available image log.

ACKNOWLEDGEMENTS

The research is supported by a VITO PhD grant nr. 1610424. The cores and geophysical well logs of the Heibaart DZH1 borehole were made available by the Geological Survey of Belgium, from the archive KBIN-BGD. In particular, Marleen De Ceukelaire and Tommy Dheuvaert are thanked for their support regarding the material. We would like to thank Prof. Ondrej Bábek, two anonymous reviewers and editor Prof. Reza Rezaee, for their detailed and constructive feedback which have significantly improved the manuscript.

APPENDICES

Appendix A

The selected geochemistry data of Muchez (1988), plotted along the depth of the borehole. The cored intervals and lithotype subdivision (fig. 2) are shown on the left.

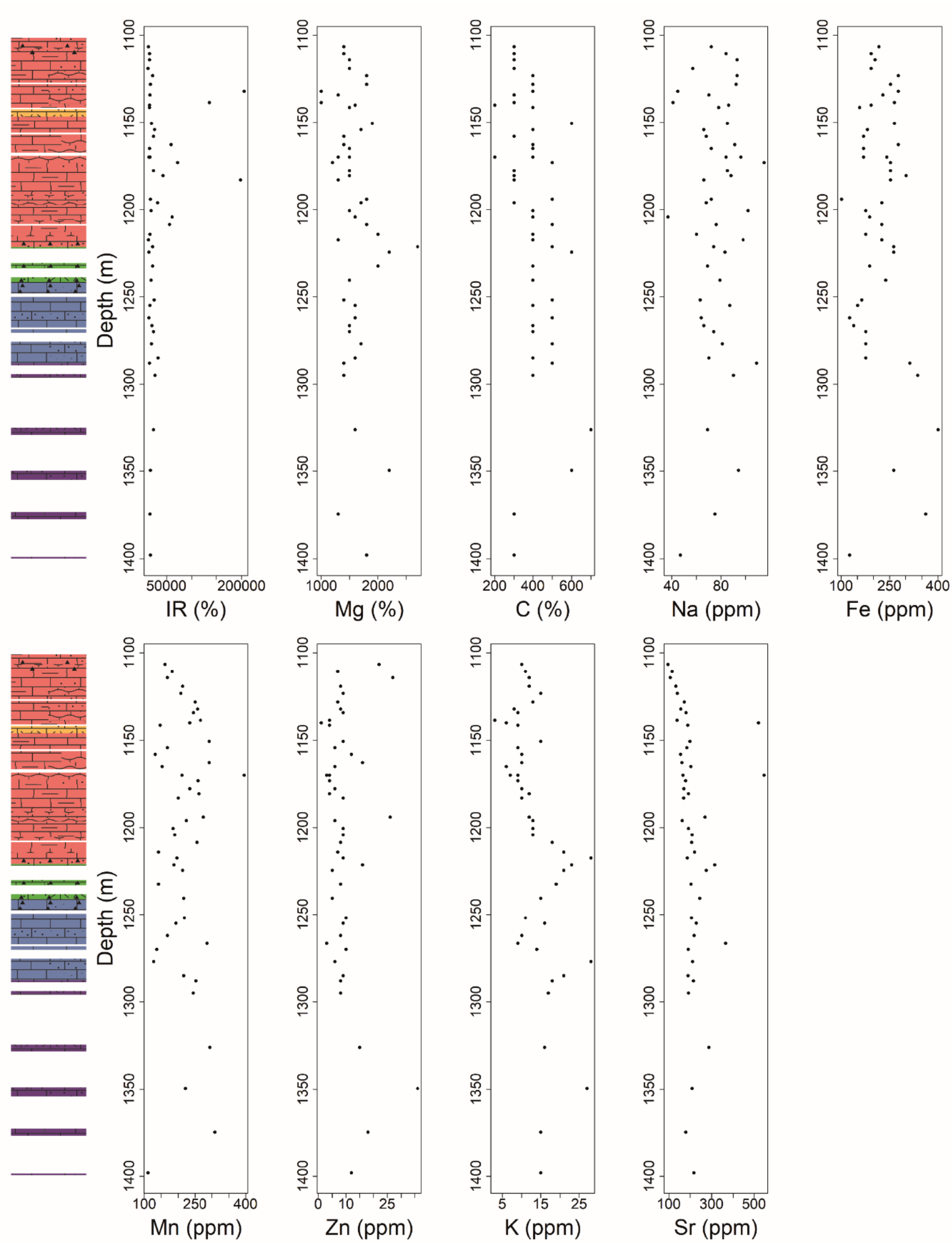

Appendix B

Geophysical well logs of the Heibaart DZH1 borehole in northern Belgium, of the Viséan interval. The cored intervals and lithotype subdivision (fig. 2) are shown on the left.

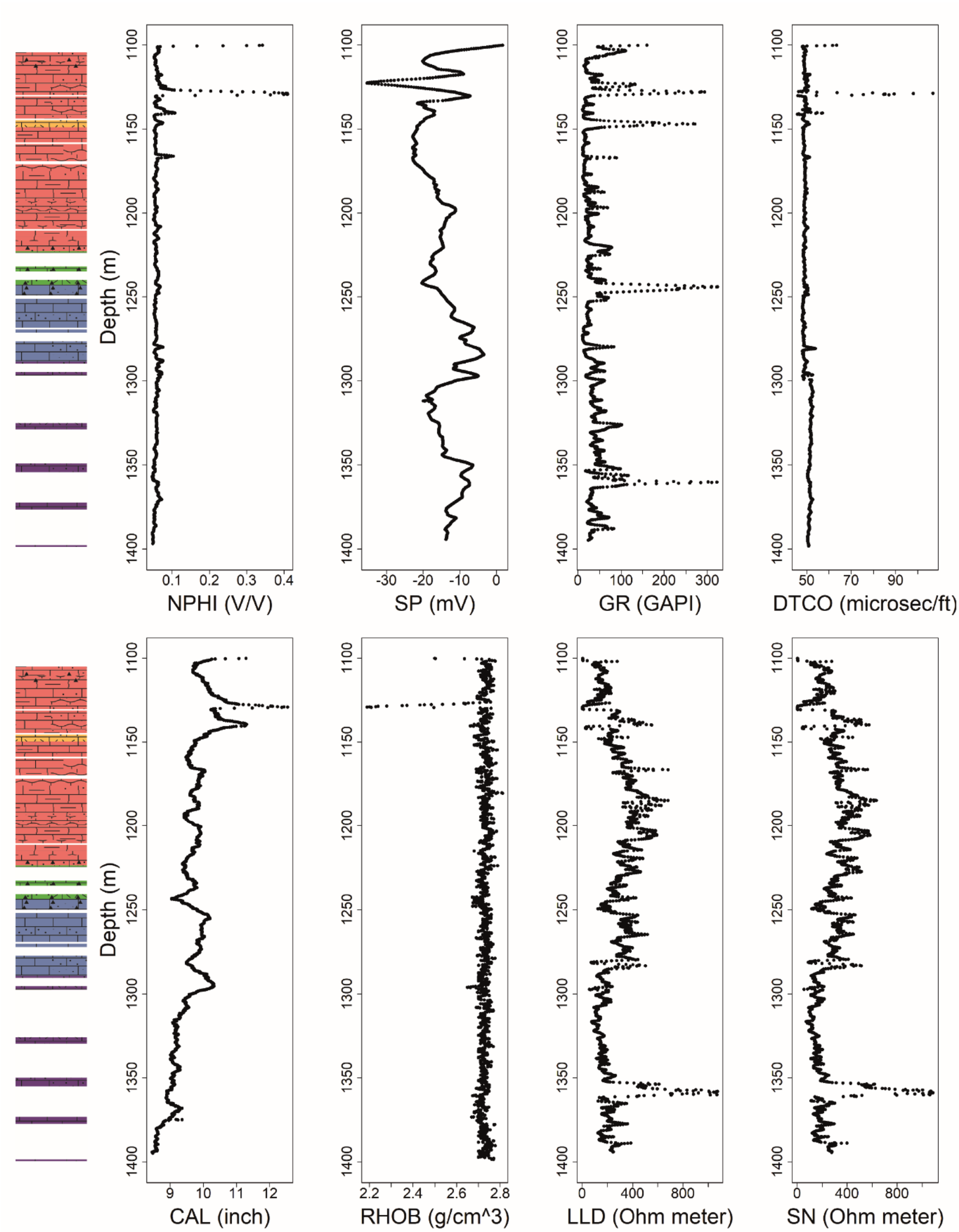

Appendix C

Results of the pairwise Wilcoxon tests of the transformed numerical variables. Variables without any significant differences among the lithotype units are not listed here (confidence level of 95%). Also, partially open vugs are only observed in lithotype unit A and therefore their frequency, aperture and open part variables were not included in the Wilcoxon tests. The y-axis of the boxplot represents the indicated transformed variable. P-values of the pairwise tests are shown in the table (in bold if lower than 0.05).

Vein frequency

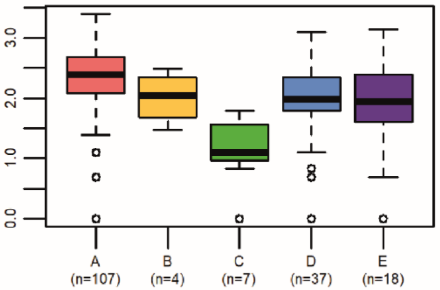

	A	B	C	D
B	0.2853	-	-	-
C	**0.0019**	0.0522	-	-
D	**0.0060**	0.9660	**0.0242**	-
E	**0.0325**	0.9660	0.0522	0.9660

A > C & D & E and D > C

Cemented vug frequency

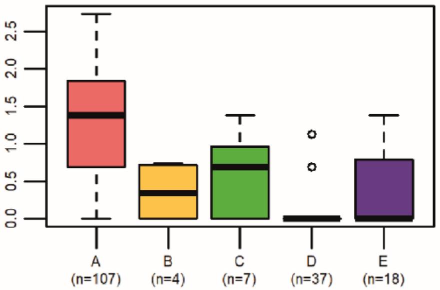

	A	B	C	D
B	0.06705	-	-	-
C	0.06705	0.61233	-	-
D	**1E-10**	**0.03669**	**0.00350**	-
E	**0.00062**	0.96183	0.55279	**0.01221**

A > E > D and B & C > D

Vein inclination

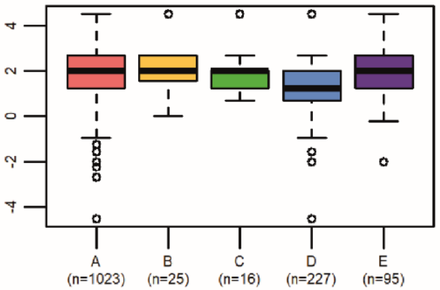

	A	B	C	D
B	0.658	-	-	-
C	0.741	0.545	-	-
D	**7.1E-09**	**0.033**	0.124	-
E	0.276	0.775	0.545	**4.2E-06**

A & B & E > D

Stylolite amplitude

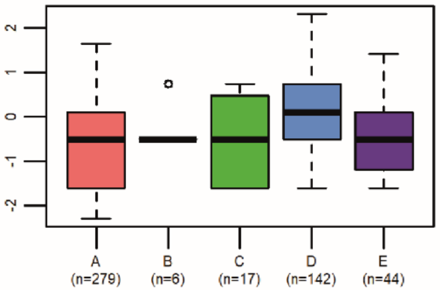

	A	B	C	D
B	0.576	-	-	-
C	0.651	0.831	-	-
D	**1.5E-08**	0.628	0.279	-
E	0.351	0.806	0.967	**0.037**

D > A & E

Stylolite inclination

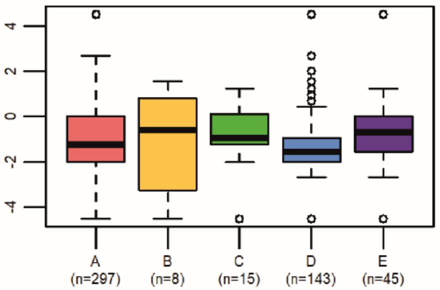

	A	B	C	D
B	0.980	-	-	-
C	0.980	0.980	-	-
D	**4E-05**	0.678	**0.021**	-
E	0.980	0.980	0.980	**0.011**

A & C & E > D

C concentration

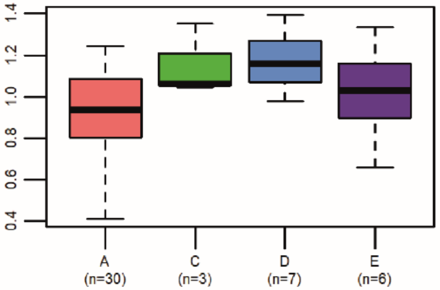

	A	B	C	D
B	-	-	-	-
C	0.39	-	-	-
D	**0.04**	-	0.83	-
E	0.63	-	0.66	0.59

D > A

Fe concentration

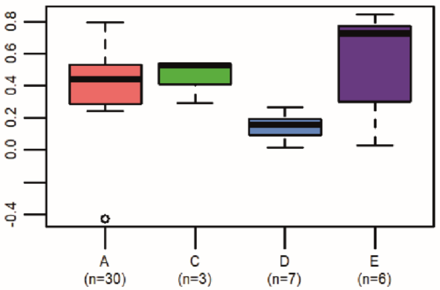

	A	B	C	D
B	-	-	-	-
C	0.61364	-	-	-
D	**0.00015**	-	0.05000	-
E	0.21951	-	0.45714	0.06993

A > D

K concentration

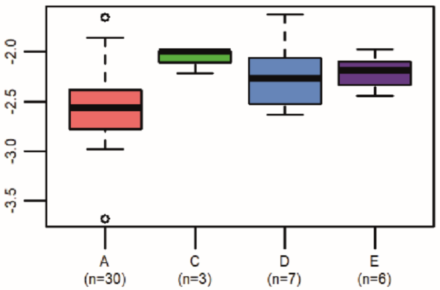

	A	B	C	D
B	-	-	-	-
C	**0.034**	-	-	-
D	0.118	-	0.657	-
E	**0.024**	-	0.657	0.731

C & E > A

Thermal Neutron Porosity log (NPHI)

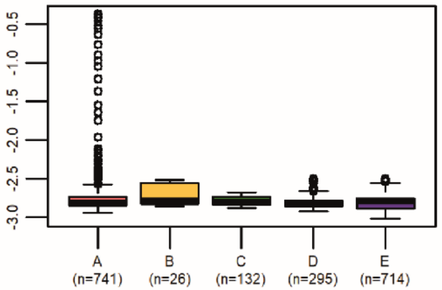

	A	B	C	D
B	0.0529	-	-	-
C	0.1038	0.1141	-	-
D	**0.0281**	**0.0042**	**0.0037**	-
E	**0.0037**	**0.0079**	**0.0042**	0.8758

A & B & C > D & E

Spontaneous Potential log (SP)

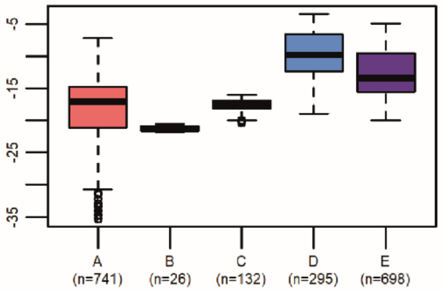

	A	B	C	D
B	**1.0E-05**	-	-	-
C	0.11	**1.1E-15**	-	-
D	**<2E-16**	**<2E-16**	**<2E-16**	-
E	**<2E-16**	**<2E-16**	**<2E-16**	**<2E-16**

D > E > A & C > B

Gamma Ray log (GR)

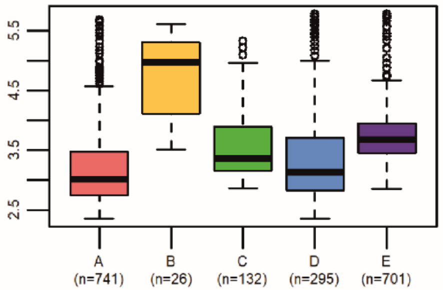

	A	B	C	D
B	**3.9E-14**	-	-	-
C	**7.2E-15**	**5.6E-11**	-	-
D	**0.0057**	**5.6E-11**	**1.1E-06**	-
E	**<2E-16**	**5.6E-11**	**1.6E-09**	**<2E-16**

B > E > C > D > A

Delta-T Compressional Log (DTCO)

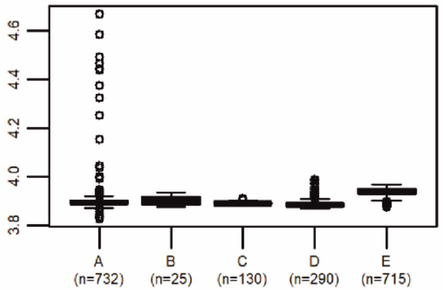

	A	B	C	D
B	0.0681	-	-	-
C	**9.8E-09**	**0.0017**	-	-
D	**<2E-16**	**0.0002**	**5.4E-09**	-
E	**<2E-16**	**2.4E-12**	**<2E-16**	**<2E-16**

E > A & B > C > D

Caliper log (CAL)

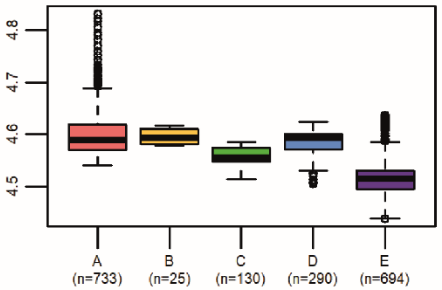

	A	B	C	D
B	0.25	-	-	-
C	**<2E-16**	**7.5E-13**	-	-
D	0.23	0.09	**<2E-16**	-
E	**<2E-16**	**4.6E-12**	**<2E-16**	**<2E-16**

A & B & D > C > E

Density log (RHOB)

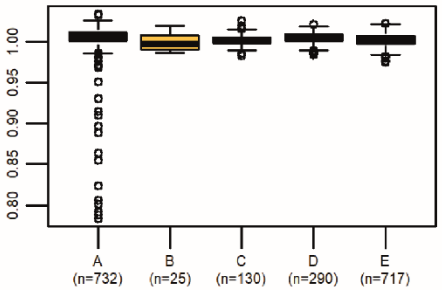

	A	B	C	D
B	**0.0051**	-	-	-
C	**2.1E-08**	0.1180	-	-
D	0.0772	**0.0104**	**2.2E-05**	-
E	**<2E-16**	0.0756	0.3464	**9.6E-07**

A & D > B & C & E

Laterolog Deep Resistivity log (LLD)

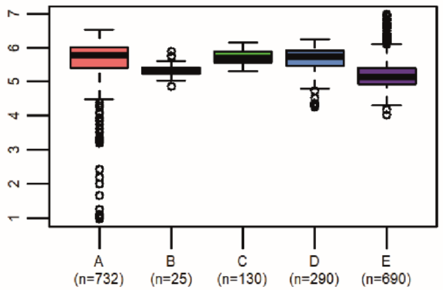

	A	B	C	D
B	**5.7E-05**	-	-	-
C	0.3837	**4.0E-09**	-	-
D	**0.0320**	**1.7E-05**	0.6101	-
E	**<2E-16**	**0.0024**	**<2E-16**	**<2E-16**

A & C & D > B > E and D > A

Short Normal Resistivity log (LLD)

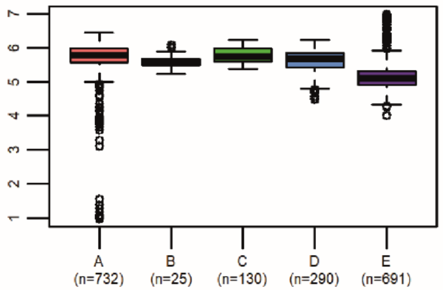

	A	B	C	D
B	**0.00507**	-	-	-
C	0.91188	**0.00087**	-	-
D	**5.4E-08**	0.40463	**2.5E-05**	-
E	**<2E-16**	**2.6E-09**	**<2E-16**	**<2E-16**

A & C > B & D > E

Appendix D

Spearman rank correlation test results. Only the significant results are shown, using a confidence level of 95%. All numerical variables were tested pairwise. The p-values (lower than 0.05) are shown in the lower left part of the table and the correlation coefficients (rho values) in the upper right part. The blue cells show correlations between variables which were averaged per meter-interval. The green cells show correlations between two variables regarding the same feature, for instance vein width and vein inclination. These variables were tested using the original data instead of the averaged data per meter-interval. Abbreviations: freq = frequency; POVein = partially open vein; Styl = stylolite; CemVug = cemented vug; POVug = partially open vug; incl = inclination; openpart = open part; ampl = amplitude; IR = insoluble residue; C = organic carbon; NPHI = Thermal Neutron Porosity; SP = Spontaneous Potential; GR = Gamma Ray; DTCO = Delta-T Compressional; CAL = Caliper; RHOB = Density; LLD = Laterolog Deep Resistivity; SN = Short Normal Resistivity.

		FREQUENCIES					FEATURE CHARACTERISTICS									
		Vein freq	POVein freq	Styl freq	CemVug freq	POVug freq	Vein width	Vein incl	POVein width	POVein incl	POVein aperture	POVein openpart	Styl ampl	Styl incl	POVug aperture	POVug openpart
FREQUENCIES	Vein freq	X	0.239		0.213		0.282									
	POVein freq	0.002	X		0.159		0.235									
	Styl freq			X		-0.166		0.156						-0.312		
	CemVug freq	0.005	0.036		X	0.180							-0.204			
	POVug freq			0.029	0.018	X						-0.340				
FEATURE CHARACTERISTICS	Vein width	2.50E-04	0.002				X	-0.076	0.318							
	Vein incl			0.045			0.005	X					-0.183			
	POVein width						0.038		X		0.742	-0.237				
	POVein incl									X				0.421		
	POVein aperture								3.71E-14		X					
	POVein openpart					0.024			0.039			X				
	Styl ampl				0.023			0.045					X			
	Styl incl			2.98E-04						0.016				X		
	POVug aperture														X	0.716
	POVug openpart														2.60E-05	X
GEOCHEMISTRY	IR															0.002
	C				0.028								0.024			
	Mg	0.005														
	Na				0.016											
	Fe			0.049						0.030			0.014			
	Mn						0.009					0.022				
	Zn															0.014
	K	0.005	0.008	0.002		0.013					0.021					
	Sr		0.036		0.022	0.004										
GEOPHYSICAL WELL LOGS	NPHI									0.015			0.031			
	SP	0.018		7.07E-08	0.001	4.92E-05							0.005	6.06E-05		
	GR				0.003	0.007										3.63E-04
	DTCO												2.76E-07	0.023		
	CAL				0.004		0.008			0.035						
	RHOB	0.002				0.018								0.033		
	LLD	0.024				0.010	0.015	0.031				0.004				
	SN	0.016					3.73E-04	0.031			0.025	0.018				

		GEOCHEMISTRY									GEOPHYSICAL WELL LOGS							
		IR	C	Mg	Na	Fe	Mn	Zn	K	Sr	NPHI	SP	GR	DTCO	CAL	RHOB	LLD	SN
FREQUENCIES	Vein freq			-0.427					-0.429			-0.181				0.231	0.173	0.185
	POVein freq								-0.405	-0.325								
	Styl freq					-0.305			0.468			0.398						
	CemVug freq		-0.339		0.369					-0.352		-0.241	-0.222		0.218			
	POVug freq								-0.382	-0.436		-0.305	-0.205			0.179	-0.196	
FEATURE CHARACTERISTICS	Vein width						0.405								0.207		0.191	0.276
	Vein incl																0.169	0.169
	POVein width																	
	POVein incl					-0.756					-0.376				-0.335			
	POVein aperture								-0.829									0.345
	POVein openpart						0.783										0.433	0.360
	Styl ampl		0.392			-0.423					-0.194	0.250		-0.440				
	Styl incl											-0.347		0.199		-0.188		
	POVug aperture																	
	POVug openpart	-0.913						0.812					0.705					
GEOCHEMISTRY	IR	X						-0.424	-0.388				-0.431				0.501	0.459
	C		X			-0.483				0.514				-0.356				
	Mg			X		-0.480	-0.331			0.517				-0.325				
	Na				X													
	Fe		0.001	0.001		X	0.461			-0.390	0.440			0.658				
	Mn			0.033		2.00E-03	X	-0.314	-0.422					0.372				
	Zn	0.006					0.044	X			-0.424				-0.349	0.338		
	K	0.012					0.006		X			0.509	0.369					
	Sr		5.85E-04	5.41E-04		0.011				X				-0.337				
GEOPHYSICAL WELL LOGS	NPHI					0.004		0.006			X		0.336	0.444	0.260	-0.358	-0.264	-0.270
	SP								6.75E-04			X	0.172					
	GR	0.005							0.017		7.14E-06	0.025	X	0.397		-0.318	-0.299	-0.283
	DTCO		0.021	0.036		4.03E-06	0.016			0.029	1.03E-09		1.01E-07	X		-0.329	-0.179	-0.213
	CAL							0.024			5.89E-04				X			
	RHOB							0.028			1.47E-06		2.26E-05	9.60E-06		X	0.301	0.316
	LLD	8.46E-04									4.76E-04		7.57E-05	0.019		6.51E-05	X	0.952
	SN	0.002									3.49E-04		1.88E-04	0.005		2.52E-05	0	X

Appendix E

List of all used numerical variables and their units, from the dataset in which the sequence is subdivided into length-intervals of one meter. The percentages of meter-intervals without data is indicated in the third column, for each variable. For instance, an interval without stylolites does not contain an average stylolite amplitude value. The geochemistry data of Muchez (1988) were used.

Variable	**Unit**	**Meter-intervals without data (%)**
Dataset 2: geochemistry		
Insoluble Residue concentration (IR)	%	76
Organic carbon concentration (C)	%	76
Magnesium concentration (Mg)	%	76
Sodium concentration (Na)	ppm	76
Iron concentration (Fe)	ppm	76
Manganese concentration (Mn)	ppm	76
Zinc concentration (Zn)	ppm	76
Potassium concentration (K)	ppm	76
Strontium concentration (Sr)	ppm	76
Dataset 3: geophysical well logs		
Thermal Neutron Porosity log (NPHI)	V/V	1
Spontaneous Potential log (SP)	mV	1
Gamma Ray log (GR)	GAPI	1
Delta-T Compressional log (DTCO)	Microsec/ft	0
Caliper log (CAL)	Inch	1
Density log (RHOB)	g/cm^3	0

Laterolog Deep Resistivity log (LLD)	Ohm meter	1
Short Normal Resistivity log (SN)	Ohm meter	1
Dataset 4: physical features from cores		
Frequencies		
Vein frequency	m^{-1}	0
Partially open vein frequency	m^{-1}	0
Stylolite frequency	m^{-1}	0
Vug frequency	m^{-1}	0
Partially open vug frequency	m^{-1}	0
Feature characteristics		
Vein width	mm	5
Vein inclination	degrees from horizontal	5
Partially open vein width	mm	75
Partially open vein inclination	degrees from horizontal	76
Partially open vein aperture	mm	75
Partially open vein open part	%	75
Stylolite amplitude	mm	28
Stylolite inclination	degrees from horizontal	25
Partially open vug aperture	mm	87
Partially open vug open part	%	88
Short Normal Resistivity log (SN)	Ohm meter	1

REFERENCES

Aitchison, J., 1986. The Statistical Analysis of Compositional Data. Chapman and Hall, London.

Alzayer, Y.A., 2018. Differential compaction fractures in carbonate mound complexes: pioneering numerical models applied to outcrops and subsurface reservoirs (Ph.D. thesis). University of Texas, Austin.

Barros-Galvis, N., Villaseñor, P., Samaniego, F., 2015. Analytical Modeling and Contradictions in Limestone Reservoirs: Breccias, Vugs, and Fractures. Journal of Petroleum Engineering 2015.

Ben-Itzhak, L.L., Aharonov, E., Toussaint, R., Sagy, A., 2012. Upper bound on stylolite roughness as indicator for amount of dissolution. Earth and Planetary Science Letters 337-338, 186-196.

Bless, M.J.M., Bouckaert, J., Bouzet, P., Conil, R., Cornet, P., Fairon-Demaret, M., Groessens, E., Longerstaey, P.J., Meessen, J.P.M.Th. , Paproth, E., Pirlet, H., Streel, M., Van Amerom, H.W.J., Wolf, M. (1976). Dinantian rocks in the subsurface North of the Brabant and Ardenno-Rhenish massifs in Belgium, the Netherlands and the Federal Republic of Germany. Mededelingen Rijks Geologische Dienst 27, 81–195.

Bless, M.J.M., Boonen, P., Dusar, M., Soille, P., 1981. Microfossils and depositional environment of late Dinantian carbonates at Heibaart (northern Belgium). Annales de la Société géologique de Belgique 104, 135-165.

Bless, M.J.M., Bouckaert, J., Paproth, E., 1983. Recent exploration in pre-Permian rocks around the Brabant Massif (BE, NL, DE). Geologie en Mijnbouw 1983.

Bons, P., Elburg, M.A., Gomez-Rivas, E., 2012. A review of the formation of tectonic veins and their microstructures. Journal of Structural Geology 43, 33–62.

Bos, S., Laenen, B., 2017. Development of the first deep geothermal doublet in the Campine Basin of Belgium. European Geologist 43, 16–20.

Bouckaert, J., 1967. Namurian transgression in Belgium. Annales de la Société Géologique de Pologne 37, 145–150.

Cooke, M.L., Mollema, P.N., Pollard, D.D., Aydin, A., 1999. Interlayer slip and joint localization in the East Kaibab Monocline, Utah: field evidence and results from numerical modelling. Geological Society, London, Special Publications 169, 23-49.

Cooke, M.L., Simo, J.A., Underwood, C.A., Rijken, P., 2006. Mechanical stratigraphic controls on fracture patterns within carbonates and implications for groundwater flow. Sedimentary Geology 184, 225-239.

Davis, J.C., 2002. Statistics and Data Analysis in Geology. Third Edition. John Wiley & Sons Inc, New York.

Deere, D. U. & Deere, D. W. (1988). The Rock Quality Designation (RQD) index in practice. In: Kirkaldie, R. (Eds.). Rock Classification Systems for Engineering Purposes. American Society for Testing and Materials, Philadelphia, pp. 91-101.

Di Naccio, D., Boncio, P., Cirilli, S., Casaglia, F., Morettini, E., Lavecchia, G., Brozetti, F., 2005. Role of mechanical stratigraphy on fracture development in carbonate reservoirs: Insights from outcropping shallow water carbonates in the Umbria-Marche Apennines, Italy. Journal of Volcanology and Geothermal Research 148, 98-115.

Dreesen, R., Bouckaert, J., Dusar, M., Soille, J., Vandenberghe, N., 1987. Subsurface structural analysis of the late-Dinantian carbonate shelf at the northern flank of the Brabant Massif (Campine Basin, N-Belgium). Toelichtende Verhandelingen voor de Geologische en Mijnkaarten van België 21.

Dubois, C., Quinif, Y., Baele, J.-M., Barriquand, L., Bini, A., Bruxelles, L., Dandurand, G., Havron, C., Kaufmann, O., Lans, B., Maire, R., Martin, J., Rodet, J., Rowberry, M.D., Tognini, P., Vergari, A., 2014. The process of ghost-rock karstification and its role in the formation of cave systems. Earth-Science Reviews 131, 116-148.

Dusar, M., Lagrou, D., Debacker, T., 2015. Boven-Paleozoïcum tot Mesozoïcum. In: Borremans, M. (Eds.). Geologie van Vlaanderen. Academia Press, Gent, pp. 58-98.

Faÿ-Gomord, O, Verbiest, M., Lasseur, E., Caline, B., Allanic, C., Descamps, F., Vandycke, S., Swennen, R., 2018. Geological and mechanical study of argillaceous North Sea chalk: Implications for the characterization of fractured reservoirs. Marine and Petroleum Geology 92, 962-978.

Ferril, D.A., Morris, A.P., McGinnis, R.N., Smart, K.J., Wigginton, S.S., Hill, N.J., 2017. Mechanical stratigraphy and normal faulting. Journal of Structural Geology 94, 275-302.

Fossen, H., 2010. Structural Geology. Cambridge University Press, New York.

Geluk, M.C., Dusar, M., de Vos, W., 2007. Pre-Silesian. In: Wong, T. E., Batjes, D. A.J., de Jager, J. (Eds.). Geology of the Netherlands. Royal Netherlands Academy of Arts and Sciences, pp. 27-42.

GEOHEAT-APP, 2014. Economical feasability of intermediate and deep geothermal energy in supplying sustainable heat for building and renovation projects. VITO, Grontmij-Nederland and TNO, Interreg Vlaanderen-Nederland. https://vito.be/nl/geoheat-app.

Graulich, J. M., 1962. La phase sudète de l’orogène varisque dans le synclinorium de Namur à l’est du Samson. Bulletin de La Société Belge de Géologie 71, 181-199.

Harings, M.J., 2014. CAL-GT-01 - Implications for the distribution of the Early Namurian Geverik Member in the Netherlands. Extended Abstract EAGE 2014.

Holland, M., Urai, J.L., 2010. Evolution of anastomosing crack-seal vein networks in limestones: Insights from an exhumed high-pressure cell, Jabal Shams, Oman Mountains. Journal of Structural Geology 32, 1279-1290.

Jacquemyn, C., Swennen, R., Ronchi, P., 2012. Mechanical stratigraphy and (palaeo)karstification of the Murge area (Apulia, southern Italy). In: Garland, J., Neilson, J.E., Laubach, S.E., Whidden, K.J. (Eds). Advances in Carbonate Exploration and Reservoir Analysis. Geological Society, London, Special Publications, pp. 169-186.

Kombrink, H., Leever, K.A., Van Wees, J.D., Van Bergen, F., David, P., Wong, T.E., 2008. Late Carboniferous foreland basin formation and Early Carboniferous stretching in Northwestern Europe: Inferences from quantitative subsidence analyses in the Netherlands. Basin Research 20, 377–395.

Laenen, B., Van Tongeren, P., Dreesen, R., Dusar, M., 2004. Carbon dioxide sequestration in the Campine Basin and the adjacent Roer Valley Graben (North Belgium): an inventory. Geological Society, London, Special Publications 233, 193–210.

Laenen, B., 2003. Lithostratigrafie van het pre-Tertiair in Vlaanderen, Deel II: Dinantiaan & Devoon. VITO report 2003/ETE/095, 90p.

Lamarche, J., Lavenu, A.P.C., Gauthier, B.D.M., Guglielmi, Y., Jayet, O., 2012. Relationships between fracture patterns, geodynamics and mechanical stratigraphy in Carbonates (South-East Basin, France). Tectonophysics 581, 231-245.

Langenaeker, V., 2000. The Campine Basin: stratigraphy, structural geology, coalification and hydrocarbon potential for the Devonian to Jurassic (Ph.D. thesis). KU Leuven.

Laubach, S.E., Olson, J.E., Gross, R., 2009. Mechanical and fracture stratigraphy. AAPG Bulletin 93, 1413-1426.

Li, Y., Schmitt, R., 1998. Drilling-induced core fractures and in situ stress. Journal of Geophysical Research 103, 5225-5239.

McCann, T., 2008. The geology of Central Europe. Volume 1: Precambrian and Palaeozoic. Geological Society, London.

McGinnis, R.N., Ferrill, D.A., Morris, A.P., Smart, K.J., 2017. Mechanical stratigraphic controls on natural fracture spacing and penetration. Journal of Structural Geology 95, 160-170.

Muchez, P., 1988. Sedimentologische, diagenetische en geochemische studie van de Dinantiaan strata ten noorden van het Brabant Massief (Bekken van de Kempen) (Ph.D. thesis). KU Leuven.

Muchez, P., Peeters, C., 1986. The occurrence of a cryptalgal reef structure in the Upper Viséan of the Visé area (the Richelle quarries). Annales de La Société Géologique de Belgique 109, 573–577.

Muchez, P., Viaene, W.A., 1990. Lithogeochemistry of the Dinantian strata of the Campine-Brabant Basin (northern Belgium). Annales de la Société Géologique de Belgique 113, 341-358.

Muchez, P., Langenaeker, V., 1993. Middle Devonian to Dinantian sedimentation in the Campine Basin (Northern Belgium): Its Relation to Variscan Tectonism. Special publications of the International Association of Sedimentologists 20, 171-181.

Muchez, P., Conil, R., Viaene, W., Bouckaert, J., Poty, E., 1987. Sedimentology and biostratigraphy of the Viséan carbonates of the Heibaart (DzH1) borehole (northern Belgium). Annales de la Société géologique de Belgique 110, 199-208.

Muchez, P., Viaene, W., Bouckaert, J., Conil, R., Dusar, M., Poty, E., Soille, P., Vandenberghe, N., 1990. The occurrence of a microbial buildup at Poederlee (Campine Basin, Belgium): biostratigraphy, sedimentology, early diagenesis and significance for early Warnantian paleogeography. Annales de La Société Géologique de Belgique 113, 329–339.

National Research Council, 1996. Rock Fractures and Fluid Flow. National Academies Press, Washington D.C.

Nelson, R.A., 1985. Geological analysis of naturally fractured reservoirs. Gulf Publishing Company, Houston, Texas.

Pendexter, C., Rohn, R.E., 1954. Fractures induced during drilling. Journal of Petroleum Technology 6, 15.

Priest, S. D. & Hudson, J. A., 1976. Discontinuity Spacings in Rock. International Journal of Rock Mechanics and Mining Sciences & Geomechanics Abstracts 13, 135-148.

Reijmer, J.J.G., Ten Veen, J.H., Jaarsma, B. & Boots, R., 2017. Seismic stratigraphy of Dinantian carbonates in the southern Netherlands and northern Belgium, Netherlands Journal of Geosciences 96, 353-379.

Sanz, P.F., Pollard, D.D., Allwardt, P.F., Borja, R.I., 2008. Mechanical models of fracture reactivation and slip on bedding surfaces during folding of the asymmetric anticline at Sheep Mountain, Wyoming. Journal of Structural Geology 30, 1177-1191.

Smart, K.J., Ferrill, D.A., Morris, A.P., 2009. Impact of interlayer slip on fracture prediction from geomechanical models of fault-related folds. AAPG bulletin 93, 1447-1458.

Swennen, R., Muchez, P., 1991. Sedimentological and diagenetic study of the Dinantian carbonates and underlying siliciclastics of Placid borehole O-18-01. www.nlog.nl.

Thorez, J., Bourguignon, P., 1973. Minéraux argilleux des argiles de dissolution des calcaires Dinantiens en Condroz. Annales de la Société Géologique de Belgique 96, 59-85.

Thorez, J., 1987. Clay mineralogy of some clayey intervals in the Thermae 2002 borehole (Valkenburg a/d Geul, the Netherlands). Annales de la Société Géologique de Belgique 110, 53-58.

Total E&P United Kingdom, 2007. A regional review of the Dinantian carbonate play: Southern North Sea & onshore UK. Report number UK-REG-0278.FH.

Toussaint, R., Aharonov, E., Koehn, D., Gratier, J.-P., Ebner, M., Baud, P., Rolland, A., Renard, F., 2018. Stylolites: A review. Journal of Structural Geology 3, 349–367.

Van Adrichem Boogaert, H. A. & Kouwe, W. F. P., 1993-1997. Carboniferous Limestone Group. In: Stratigraphic Nomenclature of the Netherlands.

Vandenberghe, N., 1984. The subsurface geology of the Meer area in North Belgium and its significance for the occurrence of hydrocarbons. Journal of Petroleum Geology 7, 5–66.

Vandenberghe, N., Poggiagliomi, E., Watts, G., 1986. Offset-dependent seismic amplitudes from karst limestone in northern Belgium. First Break 4, 9-27.

Vandenberghe, N., Dusar, M., Boonen, P., Fan, L.S., Voets, R., Bouckaert, J., 2000. The Merksplas-Beerse geothermal well (17W265) and the Dinantian reservoir. Geologica Belgica 3, 349-367.

Van Hulten, F.F.N., 2012. Devono-carboniferous carbonate platform systems of the Netherlands. Geologica Belgica 15, 284-296.

Verhaegen, J., Weltje, G.J., Munsterman, D., 2018. Workflow for analysis of compositional data in sedimentary petrology: provenance changes in sedimentary basins from spatio-temporal variation in heavy-mineral assemblages. Geological Magazine. Advance online publication. doi: 10.1017/S0016756818000584

Warren, J.E., Root, P.J., 1963. The behaviour of naturally fractured reservoirs. SPE Journal, 245-255.

Weltje, G.J., 2012. Quantitative models of sediment generation and provenance: State of the art and future developments. Sedimentary Geology 280, 4-20.

Ziegler, P. A., 1990. Geological Atlas of Western and Central Europe (2nd edition). The Hague: Shell Internationale Petroleum Maatschappij B.V.; Bath: Geological Society Publishing House.